

Seton Hall University

eRepository @ Seton Hall

Seton Hall University Dissertations and Theses
(ETDs)

Seton Hall University Dissertations and Theses

Summer 8-6-2020

Investigation of the Chemical Kinetics in an Atmospheric Cold Plasma towards CO₂ Conversion

Daniel Piatek

daniel.piatek@student.shu.edu

Follow this and additional works at: <https://scholarship.shu.edu/dissertations>



Part of the [Plasma and Beam Physics Commons](#)

Recommended Citation

Piatek, Daniel, "Investigation of the Chemical Kinetics in an Atmospheric Cold Plasma towards CO₂ Conversion" (2020). *Seton Hall University Dissertations and Theses (ETDs)*. 2800.

<https://scholarship.shu.edu/dissertations/2800>

Investigation of the Chemical Kinetics in an Atmospheric Cold Plasma towards CO₂ Conversion

by

Daniel Piatek

Submitted in partial fulfillment of the requirements for the degree

Master of Physics

Department of Physics

Seton Hall University

August 2020

©2020 Daniel Piatek

SETON HALL UNIVERSITY

COLLEGE OF ARTS AND SCIENCES

DEPARTMENT OF PHYSICS

APPROVAL FOR SUCCESSFUL DEFENSE

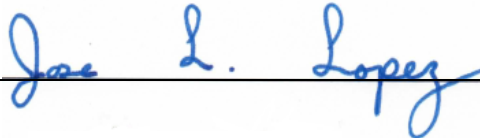
Daniel Piatek has successfully defended and made the required modifications to the text of the master's thesis for the **M.S.** during this **Summer Semester 2020**.

MASTER'S COMMITTEE

(please sign and date beside your name)

Mentor:

Dr. Jose L. Lopez



(8/3/2020)

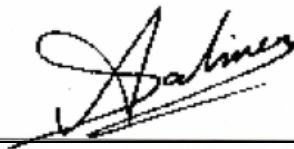
Co-Mentor:



Dr. Shurik Yatom

(8/3/2020)

Committee Member:



Dr. M. Alper Sahiner

(8/3/2020)

The mentor and any other committee members who wish to review revisions will sign and date this document only when revisions have been completed. Please return this form to the Office of Graduate Studies, where it will be placed in the candidate's file and submit a copy with your final thesis to be bound as page number two.

ACKNOWLEDGEMENTS

I would like to thank my family and especially my Mom who has been my biggest supporter. Thank you to Seton Hall University for the chance to not only earn my B.S. in physics but also an M.S. as well. I am very grateful for the opportunities this University has given me. It was an honor being the first student accepted into the M.S. in Physics program and it has been a great learning experience. Furthermore, I would like to thank my mentor Dr. Jose L. Lopez for keeping me on track during this Program. I would additionally like to thank Dr. M. Alper Sahiner, Chair of the Department of Physics at Seton Hall University for his guidance along with the support of faculty and staff of the Department. Additionally, I would like to thank my friends and colleagues at LEAP who have helped me immensely on this project. I would further like to especially thank the Princeton Plasma Physics Laboratory (PPPL) for allowing me to conduct this research at their facilities and being an amazing place to work and learn. Finally, I would particularly like to thank Dr. Shurik Yatom of PPPL for his help with this research and express my sincere gratitude to Dr. Yevgeny Raitses for his generosity to allow me to be part of this research team in the Plasma Science & Technology Department at PPPL.

TABLE OF CONTENTS

Acknowledgements.....	i
Abstract.....	iii
Introduction.....	1
Literature Review.....	20
Experimental Setup.....	23
- Reactor Design/Setup and Catalyst Preparation.....	23
- Optical Emission Spectroscopy (OES) Setup.....	28
- Gas Mixtures and Experiments.....	28
Results and Discussion.....	29
- H ₂ /N ₂ and CO ₂	31
- CO ₂ and H ₂ O.....	33
- Pure CO ₂	36
- Argon and CO ₂ with H ₂ O.....	37
- Helium/Hydrogen with CO ₂	38
- Comparison and Discussion.....	39
Conclusion.....	41
References.....	42
Appendix 1.....	45

Abstract

Hydrogenation of carbon dioxide (CO_2) to methanol (CH_3OH) is a promising route for utilization of excess and residual CO_2 . The conversion of CO to methanol is a well-developed process but the ability to use CO_2 as a feed gas still requires high pressures (30-300 atm) to attain conversion. In this work, the hydrogenation of CO_2 is explored using H_2O as well as H_2 in an atmospheric pressure nonthermal (cold) plasma created with a dielectric barrier discharge (DBD) reactor. Different gas mixtures such as argon (Ar) and helium (He) are used to understand their interactions in the process of CO_2 hydrogenation. Optical emission spectroscopy (OES) is done in this work to analyze under various voltage and frequency settings for comparison. This investigation shows that the conversion to methanol was not achieved. However, the addition of argon into the gas mixture resulted in increased dissociation of CO_2 within the plasma, which is a key step in the hydrogenation of CO_2 to methanol.

Introduction

Plasma makes up 99.9% of the visible universe. It is the most energetic state of matter. To elaborate further on this, a solid has a definite shape and volume and the particles are tightly packed together. As energy is applied, the structure between particles becomes looser and the material loses its ability to hold a definite shape but still retains its definite volume, this phase is a liquid. Adding more energy to liquid causes the particles to gain more kinetic energy and they gain the ability to move freely. This is the gas state where the particles no longer have a definite shape or volume. The required energy for state transitions is defined as latent heat. Further introduction of energy to the particles causes the electrical properties of the gas to change and a state of free moving charged particles, neutral particles, and ions is created which is the state of plasma. The stars in the sky, like the sun, are examples of plasma. Plasma is a quasi-neutral gas that contains neutral and charged particles that display a collective behavior; however plasma is an electrical conductor due to the electrons freely moving within the plasma. Electrons, neutrals, ions, radicals, and atoms are contained within a plasma.

Many forms of plasma exist but these various types of plasmas can be classified into two types: Thermal, Non-thermal. Thermal plasmas have thermodynamic equilibrium between the electron temperature and ion temperature within the plasma. This is due to the fact that electrons gain more energy, in the plasma generation process, than they lose due to collisions with neutral particles which are heavier than the electron. The temperature of the electrons and neutral particles reaches several thousand kelvin and in some instances can

become hot enough to result in thermonuclear fusion. Thermal plasmas are usually generated at high pressures along with high plasma energies in the range of 50 to 100eV(electron volts). Examples of thermal plasma are a flame and arc. Most thermal plasmas are observed in space although there are still applications on earth that include fusion reactors and particle accelerators. Due to the nature of thermal plasmas and their high electron temperatures, they have been employed to form many different types of nanoparticles and for plastic waste treatment which both require the breaking of high energy bonds.

Non-thermal plasmas, on the other hand, have a much wider range of applications. The bulk gas, in a non-thermal plasma, is typically at about room temperature while the electrons are at much higher temperature, around 10^4 K, due to their lighter mass. Since the bulk gas is typically at room temperature and at atmospheric pressure, making them easy to work with, non-thermal plasmas have been used in many applications. A non-thermal plasma can be also referred to as a cold plasma due to the electrons having much higher temperatures than the ions and neutrals in the plasma because the method used for generating the plasma does not allow for the transfer of kinetic energy between the electrons and the heavy neutral particles via collisions. Another name for a non-thermal plasma is a non-equilibrium plasma which comes from the fact that the electron temperature is much higher than the ion temperature and is not in equilibrium. The temperature of the electrons inside a cold plasma typically range from 0.01eV to 16eV. These electron temperatures are ideal for chemical reactions due to the fact that bond dissociation and ionization energies of molecules and atoms fall into this range. Cold plasmas which contain high energy electrons, can be utilized to study and discover different reaction pathways for many research areas.

Reactions that are coupled with plasma can overcome bond dissociation energies as well as even the activation energy that is required for reactions to take place. In order to create specific products from a reaction, the correct excited species within the plasma must be present which can be done by pairing it with a specific catalyst. A catalyst is a material that aids in the breaking/formation of certain bonds that are specific towards one compound.

Plasma catalysis combines the high energy electrons in plasma with the selectivity of a catalyst. The high energy species help the reactants to reach their dissociation energy or activation energy while the catalyst only permits the synthesis of certain products due to its selectivity. Plasma catalysis has already been used in many different applications including NO_x treatment, the synthesis of ammonia, methane reformation, ozone synthesis, and synthesis of hydrogen[1-2].

Plasma catalysis can be performed under various conditions and with many different types of reactor geometries and catalysts[3]. This is due to the fact that plasma catalysis is performed with an end product in mind and so reactor designs and plasma parameters are made and tailored to have the best possible chance of creating the desired product. However, there are two general configurations that these reactor designs fall into. The first is one stage plasma catalysis or sometimes also called in-plasma catalysis. This configuration places the catalyst in the glow region of the plasma. The second configuration known as two stage plasma catalysis, also called post-plasma catalysis, places the catalyst after the glow region.

Catalytic reactors are further classified based on the type of non-thermal plasma discharge that is created within the reactor where the working gas is excited by a strong electromagnetic field. Glow discharges are the most widely recognized form of non-thermal plasmas. This type of plasma is formed under low pressure conditions where two electrodes

are in a sealed glass tube and connected to a DC power supply. The cathode in the glass tube emits electrons due to secondary electron emission induced by positive ions. These glow discharges are used in neon signs and spectroscopy. The next form of plasma employed in catalytic reactors is a radiofrequency discharge. The frequency at which this type of plasma operates at is in the range of 500kHz to 300MHz. Two reactor configurations can be employed for this type of plasma; capacitively coupled plasma(RF CCP) or inductively coupled plasma(RF ICP). Both setups utilize a quartz or steel chamber that is surrounded by RF coils. In the ICP setup, the coils are not in direct contact while in the CCP setup, the electrodes are in contact with the working gas. ICP reactors are typically used for chemical synthesis and material fabrication while the CCP reactors are used in plasma torches and atomizers. ICP discharges have lower electric fields than their CCP counterparts. This difference in electric field strength allows for the CCP to generate non-thermal plasma, at moderate pressures, while the ICP discharge at similar conditions would result in a thermal plasma. Arc discharge reactors are the next type. This kind of discharge is produced when the gap between two electrodes is quite small and a high current is allowed to flow between them in a strong electric field. The current can be anywhere from a few amps to hundreds of amperes. These plasmas are utilized in the fabrication of nanoparticles such as carbon nanotubes and boron nitride nanotubes. Following the arc discharge, the corona discharge is next type of plasma employed in plasma catalysis. The non-thermal corona discharge operates at atmospheric and high pressures and forms in regions of sharp non-uniform electric fields near the electrodes which occur at sharp edges or points. The current in these discharges reaches up to a few microamperes. This discharge is utilized in polymer treatment, water treatment, and air ionizers[4].

One of the most attractive types of plasma reactors, and the focus of this paper, for industrial use is the dielectric barrier discharge (DBD) reactor[4]. This type of discharge is created by applying an AC(alternating current) high voltage between two electrodes that are separated by a dielectric material. These discharges are operated in the frequency range of 0.05 kHz to 500kHz and the applied voltage ranges from 1-100kV_{rms}. DBD reactors operate at atmospheric pressure which eliminates the need for high pressure equipment and makes them quite appealing for industrial applications. The electron temperature and gas temperature inside a DBD, at atmospheric pressure, are lower than that of a MW or RF discharge. The micro-discharges, formed in the discharge zone between electrodes, create points of non-uniform, stronger, electric fields which increase the interaction between the catalyst and the plasma species. These non-uniform electric fields can be stronger by a factor of 10-250 and this allows the plasma to reach a non-equilibrium state. Below in Figure 1 is a diagram of a typical DBD setup.

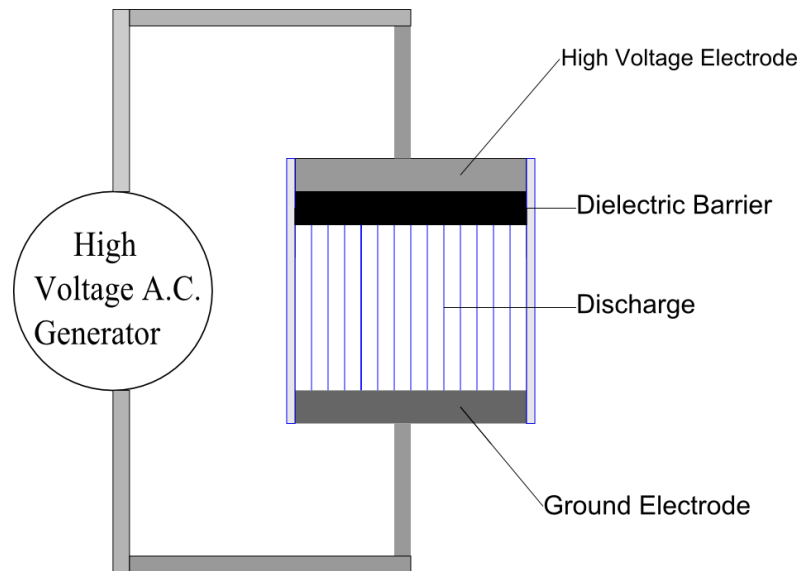


Figure 1. Diagram of a typical DBD setup [5]

Dielectric barrier discharges (DBD) have been used in various applications. They have been employed in pollution control by cleaning exhaust fumes from CO and NO_x and also in sterilization of biomedical equipment as well as in plasma televisions[7]. These various applications that DBD's have been used in are all a result of the versatility in the design of a DBD. The designs in literature are innumerable. The electrode can be made of any conducting material. The discharge gap is one of the main variables that influence the plasma characteristics. The discharge gap must be carefully designed as it will dictate whether a glow discharge or arc is formed in the gap. The arrangement of the electrodes also has a direct impact on plasma characteristics. These electrodes may be arranged concentrically, coaxially, in parallel, and in a floating electrode configuration. Various geometries have been developed to accommodate for a wide range of applications and each design is typically application specific.

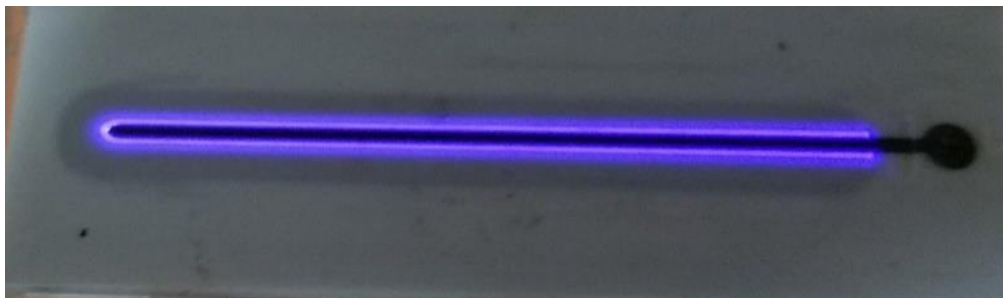
Plasma catalysis typically utilizes the concentric DBD arrangement[4]. The material for the catalyst is typically an insulator as the catalyst affects the electric field in the discharge. The method of packing the catalyst in the reactor also influences the plasma characteristics. The most used type of plasma reactor with a catalyst in it is called a packed-bed DBD reactor. These packed-bed DBD reactors have been typically packed with small round beads that are coated in a catalytic material. The round bead is chosen to increase the surface area of interaction between the plasma and the catalytic material. The addition of the catalyst also changes the discharge from streamers propagating in the gas phase to a combination of streamers and surface discharge. In a DBD, the streamer is a result of electron avalanches. The formation of the streamers causes an increase in the localized electric field

which increases the probability of molecules getting vibrationally excited. The formation of these streamers is dictated by whether the conditions in the plasma satisfy the meek criterion. The meek criterion states that in order for streamers to form between two electrodes the avalanche amplification parameter αd must exceed 20. In this equation, α is the ionization coefficient and d is the discharge gap distance. This means that the electron density must be higher than $3 \times 10^8 \text{ cm}^{-3}$:

$$N_e = \exp(\alpha d) \approx 3 * 10^8$$

Eq. 1.1

Another commonly used DBD configuration in plasma catalysis is the Surface DBD plasma reactor. In this setup, the two electrodes are positioned on both sides of a dielectric material. The high voltage electrodes is exposed to the gas while the ground electrode is covered by an insulator. The ground is covered to prevent plasma formation on both sides of the dielectric. This surface DBD configuration has been shown to have higher conversion efficiencies in certain applications. Figure 2 below shows an example of a surface discharge operating and a schematic of a surface DBD as well.



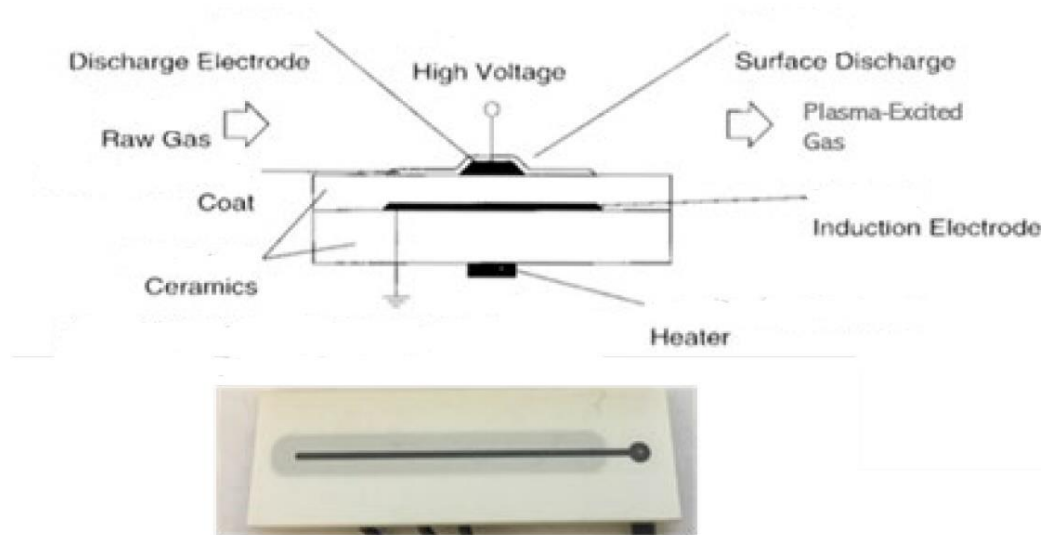


Figure 2. A surface DBD operating in atmosphere and schematic (created by Daniel Piatek)

To further understand plasma, one must understand the mechanisms, laws, and conditions that must be satisfied for the formation and propagation of plasma. Plasma is defined by the movement and interaction of neutrals and charged particles. This movement of charged particles leads to the formation of electromagnetic fields and Coulombic forces. The formation of these fields and forces focuses the charges to a range called the Debye length, λ_D . Outside of the Debye length, everything is electrically neutral while inside it is not. The Debye length is defined mathematically as:

$$\lambda_D = \left(\frac{\epsilon_0 k T_e}{n_e e^2} \right)^{1/2} \quad \text{Eq. 1.2}$$

$$L \gg \lambda_D$$

In this equation, ϵ_0 is the permittivity of free space, k is the Boltzmann constant (1.38×10^{-23} J/K), T_e is the electron temperature, n_e is the electron density, e is the charge of an electron, and L is the dimension of the plasma that must be much greater than the Debye length. The Debye length represents a charge carrier's electrostatic effect and how far that electrostatic effect persists in the plasma. The value of λ_D is also the radius of the Debye sphere. The Debye sphere is the volume, where various charged particles reside, there is influence over. Additionally, there must be a very large number of electrons within the sphere.

$$n_e \lambda_D^3 \gg 1$$

Eq. 1.3

This decreases the distance between electrons to be smaller than the Debye length. This leads to looking at the time domain of the plasma which needs to be:

$$\omega\tau \gg 1$$

Here, τ is average time that an electron spends in between collisions with neutrals while ω is the angular frequency of plasma oscillations.

The primary energy carriers in a plasma are the electrons which then also provide this energy to other particles. Electrons are the first to receive energy due to their very low mass, $m_e=9.11 \times 10^{-31}$ kg, and this also allows them to have very high mobility. Once the electron has had this energy imparted onto it, it can transfer this energy to other neutral particles via collisions which would result in many different processes such as excitation, ionization, and dissociation. In order for these processes to occur, the energy the electron is

carrying must be a specific amount however, not all electrons are excited equally and some have higher energies than others. This means that there is a distribution of energies for these electrons and a probability for them to have a specific amount of energy for a given process. This is known as the electron energy distribution function. Depending on the conditions in a given plasma, such as gas composition and pressure, this electron energy distribution function will vary but can most commonly be defined by the Maxwell-Boltzmann distribution function:

$$f(\varepsilon) = 2 \sqrt{\frac{\varepsilon}{\pi(kT_e)^3}} e^{-\frac{\varepsilon}{kT_e}} \quad \text{Eq. 1.4}$$

In this equation, T_e is the electron temperature and k is the Boltzmann constant. It is important to note that if T_e is given in electron-Volts (eV) then the Boltzmann constant becomes 1 and may be taken out of the equation. The mean electron energy for this distribution is proportional to the temperature of the electrons as follows:

$$\langle \varepsilon \rangle = \int_0^{\infty} \varepsilon f(\varepsilon) d\varepsilon = \frac{3}{2} T_e \quad \text{Eq. 1.5}$$

When an electron has enough energy to ionize an atom, a positive ion can be formed. Ions, when compared to electrons, are much heavier particles. They are unable to take in energy from an applied electric field like the electrons do because of their collisions and exchange of energy with other particles inside the plasma. In non-equilibrium plasmas, the

methods of energy transfer in the case of positive ions usually creates an energy distribution function that is similar to the Maxwell-Boltzmann function. The ion temperatures (T_i) are almost the same as the temperature of the neutral gas (T_0). For an electron to ionize a molecule or atom, it must have a sufficient amount of energy required to for the specific atom/molecule to lose an electron. A high amount of energy is required to achieve this and usually marks the upper limit of the energy exchange within the plasma.

Negative ions can also be formed inside a plasma. They can be usually formed in recombination processes or through electron attachment following dissociation[7]. Just like their positive counterparts, negative ions are heavy in relation to electron and as such are not able to take in energy from an applied electric field. They have energy distribution functions similar to that of the Maxwell-Boltzmann energy distribution function. The attachment of an electron to an atom or molecule is directly related to that atom or molecule's electron affinity. Electron affinity is the bonding energy between an electron and atom/molecule. Higher electron affinities mean that atoms/molecule will want to attach to a free electron more. The halogens are an example of elements with high electron affinities.

So far, this paper has discussed ionization, excitation, and dissociation which are examples of inelastic collisions where electrons that have gained kinetic energy and transferred it to the internal degrees of freedom of molecules (translational, vibrational, and rotational) and atoms (translational). The formation of positive ions through ionization and the formation of negative ions through recombination and attachment have also been discussed. All of these are elementary processes that occur within a plasma. All these processes are governed by the cross section, mean free path, interaction frequency reaction rate, and reaction rate coefficient[7].

The cross section of a particles is the area, centered on one particle, which another particle must be within in order for an elementary process to occur. These cross sections depend on the energies of the colliding species. For example, if one particle in a collision has a lot of energy, the cross section of that particle may decrease due to the lower probability of interacting due to the short amount of time for interaction. When a particle travels through the cross section of another particle, an elementary process results from this. The mean free path describes the average distance particle “A” will travel between successive collisions or interactions with particle “B”[7]. This relation is defined as:

$$\lambda = \frac{1}{n_B \sigma} \quad \boxed{\text{Eq. 1.6}}$$

Where n_B is the number density of particles B and σ is the cross section of particle “B”. In the mean free path λ , the particle “A” goes through, the combined mean free path and cross section, the cylindrical volume of $\lambda\sigma$ and a reaction will occur if there is at least one of particle “B” present in that volume which means $\lambda\sigma n_B=1$. The interaction frequency ν , taking into account the velocity distribution function $f(v)$ and dependence of the cross section σ on the particle’s velocity, of particle “A” with another particle “B” can be defined as:

$$\nu_A = n_B \int f(v) \sigma(v) v dv = \langle \sigma v \rangle n_B \quad \boxed{\text{Eq. 1.7}}$$

The reaction rate is the number of elementary processes that occur in a unit of volume per unit time. In order to calculate the reaction rate, the number densities and interaction frequency of the colliding partners are multiplied together and gives:

$$\omega_{A+B} = \langle \sigma v \rangle n_A n_B \quad \boxed{\text{Eq. 1.8}}$$

$$k_{A+B} = \int f(v) \sigma(v) v dv = \langle \sigma v \rangle \quad \boxed{\text{Eq. 1.9}}$$

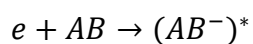
Here, the reaction rate is k and this equation takes into account the velocity distribution function as well as the cross sections of the colliding partners. Equation 1.9 is for bimolecular reactions but it can be modified to account for mononuclear reactions as well as three-body processes into the following form:

$$\omega_A = k_A n_A \quad \boxed{\text{Eq. 1.10}}$$

$$\omega_{A+B+C} = k_{A+B+C} n_A n_B n_C$$

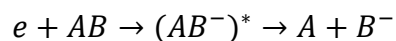
Usually in order for positive ions to form, an electron with an energy value that is equal to or greater than the ionization energy I to knock an electron from an atom/molecule[7]. However, there are other methods of ionizing an atom and generating positive ions. One method is the Penning Ionization Effect. In this type of ionization, when the electron excitation energy of a metastable atom is higher than the ionization potential of another atom, the collision between those two atoms may result in ionization of the second atom. The cross sections of this process is quite large ($\sim 10^{-15} \text{cm}^2$) which in turn leads to a higher probability of interaction between the metastable atom and another particle.

The generation of negative ions also has more than one method. One process in particular is called dissociative electron attachment. In this scenario, an electron will collide with a molecule. Molecular vibrations occur at a time scale of 10^{-14} to 10^{-13} s while the time for the interaction of a colliding electron and molecule is about 10 to 100 times quicker. Due to this, the heavy molecules are practically not moving in relation to the electron and are only stimulated by the impact of the electron. This phenomena from the time disparity is called the Franck-Condon principle. Once impact occurs, the colliding electron then attaches to the molecule and puts it into an intermediate excited state:



Eq. 1.11

The resulting excited state of the molecule is unstable and leads to two options: the molecule dissociates and the electron attaches to one of the atoms or the excited state reverts and leaves a stable molecule with a free electron. If the molecule dissociates the process becomes unbalanced. This means that the dissociative attachment process is a resonant reaction which requires the colliding electron to possess the exact amount of energy in order to not revert into a free electron and stable molecule. This is determined by the amount of potential energy gained by the molecule after the collision with the electron. If the potential energy of the non-excited molecule is higher than the intermediate step, it will continue to dissociate and become:



Eq. 1.12

The maximum cross section from this process is:

$$\sigma_{d.a.}^{max} \approx \sigma_0 \sqrt{\frac{m(M_A + M_B)}{M_A M_B}} \quad \text{Eq. 1.13}$$

Here, σ_0 is the gas kinetic cross section and m is the mass of the electron. In order for this process to occur, the electrons must have more energy than the difference between the molecules electron affinity and the dissociation energy. Because this process is resonant in nature, the estimated dissociative attachment rate coefficient is proportional to the electron temperature as shown below:

$$k_a(T_e) \approx \sigma_{d.a.}^{max}(\epsilon_{max}) \sqrt{\frac{2\epsilon_{max}}{m} \frac{\Delta\epsilon}{T_e} \exp\left(-\frac{\epsilon_{max}}{T_e}\right)} \quad \text{Eq. 1.14}$$

An electron can not only cause ionization and dissociation in a collision with an atom or molecule, it can excite them electronically, vibrationally, or rotationally[7]. Vibrational and rotational excitation can only occur in molecules due to the degrees of freedom. During electronic excitation, a particle may be excited to a resonance excited state in which the particle could de-excite via spontaneous transitions and photons emissions. However, a particle can be excited by an electron into a state where the spontaneous radiative transition to the ground state is not possible, this is a metastable excited state. Particles in this state can de-excite via collisions with other species in the plasma as well as via radiation. Metastables have a quite long lifetime which may last seconds up to minutes. These metastables can be generated in a discharge and then de-excite through specific collisions allowing for certain reactions to occur.

Molecules allow for vibrational excitation due to their added degrees of freedom. Vibrational excitation is one of the most important phenomena to understand as the discharge energy is transferred electrons to modes of molecular vibration. The Morse potential dictates the potential curve in diatomic molecules and is:

$$U(r) = D_0[1 - \exp(-\alpha(r - r_0))]^2 \quad \text{Eq. 1.15}$$

Here, r is the distance separating atoms in a diatomic molecule. The variables r_0 , α , and D_0 are referred to as the Morse potential parameters. r_0 is the equilibrium distance in between nuclei of the molecule, α is the force coefficient of interaction between nuclei, and D_0 is called the dissociation energy for a diatomic molecule with respect to minimum energy. Even though the degrees of freedom for molecules may not always be harmonic, the energy of the discrete vibrational levels can be calculated using:

$$E_v = \hbar\omega \left(v + \frac{1}{2} \right) - \hbar\omega x_e \left(v + \frac{1}{2} \right)^2, x_e = \frac{\hbar\omega}{4D_0} \quad \text{Eq. 1.16}$$

In order to account for anharmonicity of a diatomic molecule, x_e is used with a typical value of 0.01. Additionally, the distance between the vibrational quantum levels can be accounted for which especially has an impact in anharmonic oscillators where the distance between vibrational levels is not equal and decreases as the vibrational quantum increases. The last two vibrational levels have the smallest energy difference between them. This is represented by:

$$\Delta E_v = E_{v+1} - E_v = \hbar\omega - 2x_e\hbar\omega(v + 1) \quad \boxed{\text{Eq. 1.17}}$$

The rotational energy of a diatomic molecule is not affected by harmonic/anharmonic problems. It can be calculated using the Schroedinger equation as a function of rotational quantum number:

$$E_r = \frac{\hbar^2}{2I}J(J + 1) = BJ(J + 1) \quad \boxed{\text{Eq. 1.18}}$$

$$I = \left[\frac{M_1M_2}{M_1 + M_2} \right] r_0^2 \quad \boxed{\text{Eq. 1.19}}$$

Here, I is the momentum of inertia of the diatomic molecule which accounts for the two masses of the molecule. B is the rotational constant. Both of these values are heavily influenced by r_0 which is distance between the nuclei during molecular vibration. To calculate the rotational constant, the equation below can be used:

$$B = B_e - \alpha_e\left(v + \frac{1}{2}\right) \quad \boxed{\text{Eq. 1.20}}$$

In this equation, B_e is the zero vibrational level and α_e describes the effect of molecular vibration on the momentum of inertia and rotational constant.

As mentioned earlier, various forms of power can be used to generate a plasma such as AC, DC, RF, etc. These different forms of power all produce a plasma by creating an electric field. Once the electric field is high enough, the electrons acquire more energy from the electric field than they lose in collisions with neutral particles. The electrons accelerate and

eventually cause an electron avalanche. This avalanche is caused by electrons colliding with neutral atoms, ionizing those atoms, which in turn releases additional electrons that are accelerated by the electric field and collide with even more neutral atoms. This electron avalanche is described by the Townsend breakdown mechanism where the ionization coefficient α is related to the ionization rate coefficient $k_i(E/n_0)$ and electron drift velocity as follows:

$$\alpha = \frac{v_i}{v_d} = \frac{1}{v_d} k_i \left(\frac{E}{n_0} \right) n_0 = \frac{1}{\mu_e} \frac{k_i(E/n_0)}{E/n_0} \quad \boxed{\text{Eq. 1.20}}$$

Here, v_i is the ionization frequency, v_d is the electron drift velocity, μ_e is the electron mobility. The electron mobility is inversely proportional to the pressure. Another important parameter γ , which is the secondary electron emission coefficient, must be accounted for. The secondary electron emission coefficient is the probability of a secondary electron being generated on the cathode by ion impact. Every primary electron generated near the cathode produces $\exp(\alpha d - 1)$ positive ions in the gap where these positive ions move towards the cathode and eliminate $\gamma^*(\exp(\alpha d) - 1)$ electrons from the cathode. γ is heavily dependent on the type of material, gas, and ion energy.

It is important to note that different pressures require different electric field values to initiate breakdown of a gas. This can be calculated using Paschen's Law which allows one to calculate the required voltage for a gas between two electrodes to initiate breakdown as a function of pressure (Torr) and gap distance(cm):

$$V = \frac{B(pd)}{C + \ln(pd)} \quad \boxed{\text{Eq. 1.21}}$$

$$C = \ln(A) - \ln \ln \left[\frac{1}{\gamma} + 1 \right] \quad \boxed{\text{Eq. 1.22}}$$

Here, A and B are values that are known for specific gas compositions and relate to the excitation and ionization energies. Once the breakdown voltage is achieved, the gas becomes conductive. The primary avalanche then forms a thin channel known as a streamer. The direction of the streamer depends on the discharge gap. The streamer first forms at the anode, the region with the strongest electric field due to the concentration of positive charges there, and then propagates quickly towards the cathode. Plasma densities at the head of the streamer are usually in the region of 10^{12} - 10^{13} cm⁻³.

Literature Review

The conversion of CO₂ in a DBD setup has been studied by Bogaerts *et al.* [8] to understand the possible reaction mechanism and resultant products that may occur in this type of plasma. A model was developed with a focus on pure CO₂ splitting as well as a mixture of CO₂/H₂O and studied the plasma chemistry occurring within a DBD plasma. The electron temperature in the model was 2.6 eV which is typical for microdischarge filaments. It was found that electron impact dissociation contributed the most (52%) to CO₂ splitting followed by ionization (29%), dissociative ionization (16%), and dissociative attachment (23%). Under DBD conditions, it was determined that 94% of the CO₂ splitting was achieved from the ground state while only 6% results from vibrationally excited levels. This is due to the fact that the electron temperature is too high for efficient vibrational excitation of CO₂. The mixture of CO₂/H₂O was studied with a CO₂ gas flow rate of 600 mL/min and corroborated with experimental data. The water vapor content was up to 8% in the plasma. The main products formed in this mixture were CO, H₂, O₂, and H₂O₂ with no methanol formation detected. The reaction between CO and OH was found to be the most important as it controls the ratio of conversion between CO₂ and H₂O. The dissociation of CO₂ and H₂O leads to produce CO and OH however, these will quickly recombine back into CO₂ and H₂O. It was found that CO₂ conversion dropped when increasing the H₂O content. This is explained by the fact that electron impact dissociation is the major loss mechanism for CO₂ in a DBD and combined with the back reaction when H₂O is added to the system, explains this.

The addition of Ar and He into a CO₂ DBD plasma has been explored by Ramakers *et al.*[9] to understand their impact on CO₂ conversion. The experiments were carried out in a cylindrical DBD reactor with the total gas flow being kept at 300 mL/min. The Ar and He fractions

were varied from 5% to 95%. The power was set to 80W while the frequency was kept at 23.5 kHz. It was shown that upon the addition of either Ar or He, the conversion of CO₂ was increased. The addition of Ar or He up to 70% of the of the gas mixture showed similar effects on the conversion of CO₂ however, above 70% the effect became more pronounced with Ar than He. A conversion rate of 41% was achieved in the 5/95 CO₂/Ar gas mixture versus a 25% conversion rate in the 5/95 CO₂/He gas mixture. It was also found from the Lissajous figures that the breakdown voltage in the Ar/CO₂ gas mixture was significantly lower than in the He/CO₂ gas mixture. This suggests that more of the applied power can be used for CO₂ conversion and explains why the conversion is much higher with the addition of argon. Furthermore, the electrical capacitance of the plasma became comparable to the dielectric's capacitance when argon and helium are added into the system indicating the discharge gap is more fully filled with plasma which also enhances the conversion of CO₂.

The use of Cu promoted In₂O₃/TiO₂ as a photo-catalyst has been explored by Tahir *et al.*[10] on the conversion of CO₂ with H₂O and H₂. The photocatalytic reduction of CO₂ with H₂O was carried out in a photoreactor system with a total volume of 108 cm³. The light source utilized was a 500 W Hg lamp with a maximum intensity at 365 nm. The CO₂ was flown at 20 mL/min through a water bubbler. It was found that upon the addition of even 0.5% Cu onto the In₂O₃/TiO₂ promoted CH₃OH production inside the photoreactor. Furthermore, the role of using H₂O and H₂ as a reductant in these reactions was investigated. It was found that the use of H₂ reduced the production of CH₄ and the use of H₂ with H₂O has the most promising results for CO₂ conversion. Cu promoted In₂O₃/TiO₂ was compared against Ni-doped In₂O₃/TiO₂ to compare the two catalysts and it was found that the Cu promoted catalysis was more favorable for methanol production. A reaction mechanism was proposed for the conversion of CO₂ to methanol. The electrons and holes

are generated in the TiO_2 surface. The holes are able to oxidize H_2O or H_2 while the photoexcited electrons will reduce CO_2 to form CO , CH_4 , and CH_3OH .

In this project, we will be building on the findings that were reported in references [8-10]. Similarly to reference [8] CO_2 will be used as the main working gas along with water vapor in order to research CO_2 conversion to methanol in a cold plasma. Additionally, argon and helium will be added into the plasma discharge, as was reported in reference [9], in order to explore their impact on this conversion process and plasma characteristics. Suitable catalytic materials will also be explored in this project as was reported in reference [10]. Lastly, I will be adding to this area of research by investigating the impact of different applied voltages, frequencies, and flow rates on the CO_2 to methanol conversion process.

Experimental Setup

Reactor Design/Setup and Catalyst Preparation:

A surface DBD reactor was made for this experiment. It was constructed out of polycarbonate with a fused silica window to allow for OES measurements of the plasma discharge to be taken. Figure 3 shown below shows the reactor filled with the catalyst.

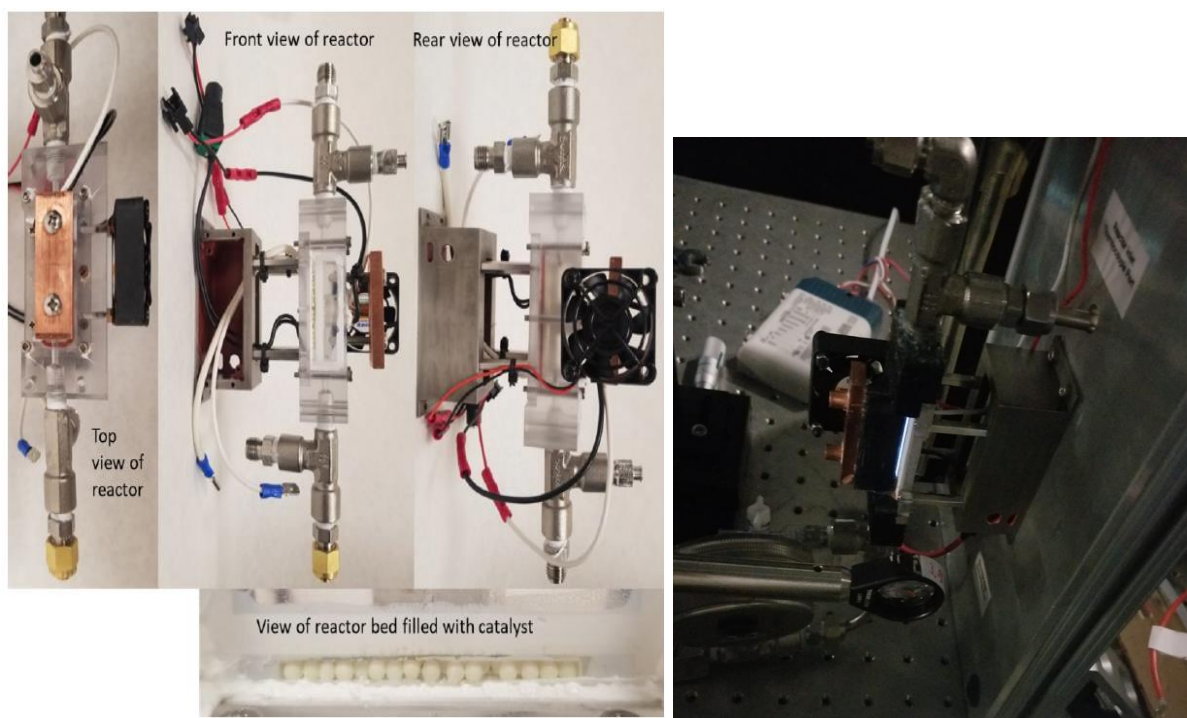


Figure 3. View of reactor filled with catalyst and reactor generating plasma (photo by Daniel Piatek)

NPT fittings were installed into the polycarbonate reactor for gas connections. The fused silica window was sealed using silicone. The UV LED, Chanzon 10W, is installed directly above the surface DBD and has a copper heat sink attached on top with a fan for cooling purposes. The

total reactor volume was calculated to be $2 \times 10^{-6} \text{m}^3$. The peak emission wavelength of the LED is shown in Figure 4 below. The emission of the UV LED is centered on the 365 nm wavelength.

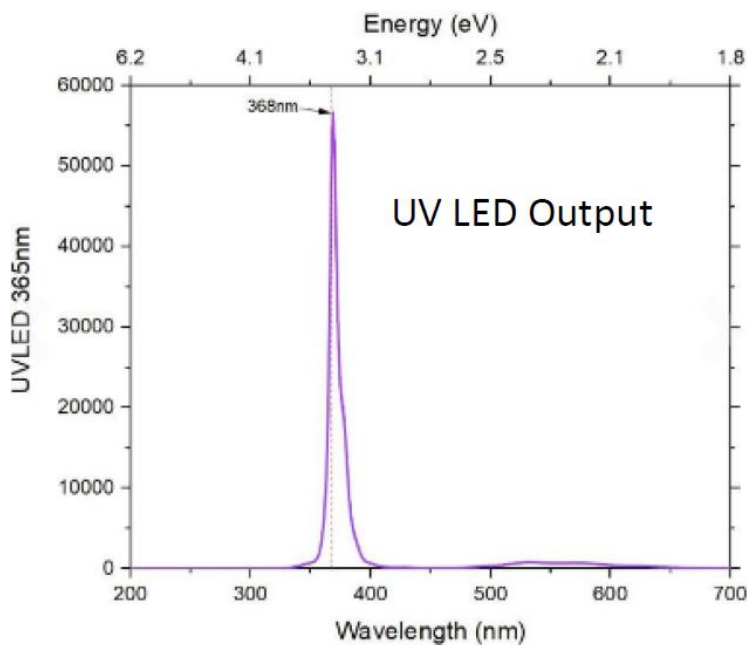


Figure 4. Peak wavelength of emission for UV LED. (photo by Daniel Piatek)

The surface DBD itself is a single electrode design with the grounding electrode buried inside the ceramic dielectric material. The working gas flows over the high voltage electrode. A schematic of the surface DBD chip as well as the surface DBD generating a plasma is presented in Figure 5.

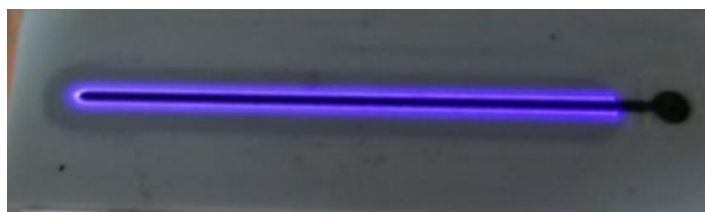
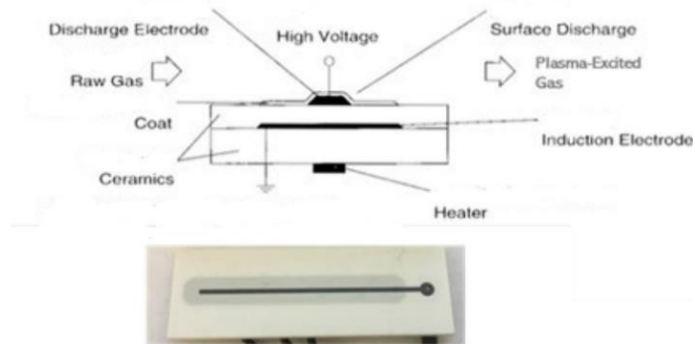


Figure 5. Schematic of surface DBD chip and plasma generated. (created by Daniel Piatek)

The catalyst used was In_2O_3 impregnated yttrium stabilized zirconia (YSZ) beads. The YSZ beads were heat treated and impregnated with indium nitrate and then heat treated to form indium oxide. A picture of the catalyst is presented in Figure 6.



Figure 6. In_2O_3 impregnated YSZ beads. (photo by Daniel Piatek)

The gas was fed into the reactor using two flow controllers, Cole Palmer PMR1-010352 and Cole Palmer PMR1-010351 as shown in figure 7 below.

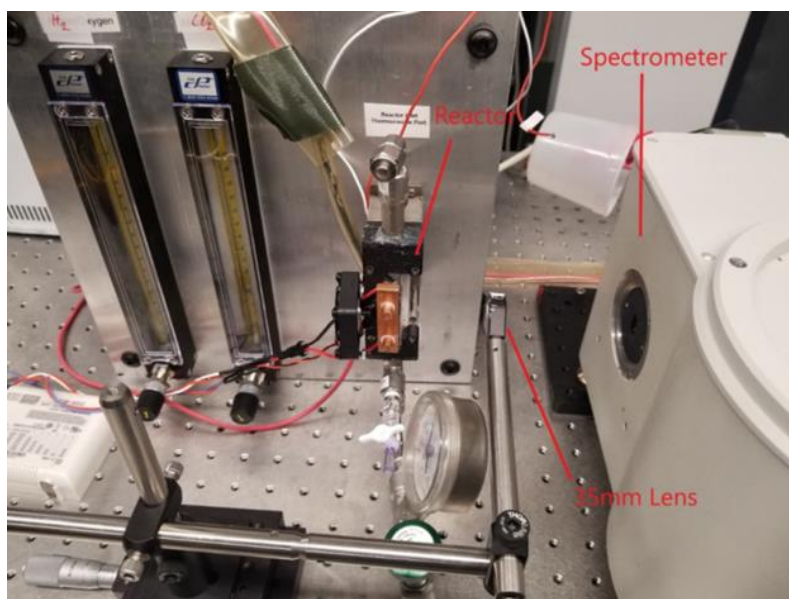


Figure 7. Reactor in experimental setup with flow controllers and focusing lens aligned with spectrometer slit. (photo by Daniel Piatek)

Humidity was introduced to the reactor by flowing the CO₂ gas through a bubbler which is shown in figure 8. The reactor was flushed for 30 minutes with CO₂ before conducting experiments in order to ensure no outside gases were present. The amount of water vapor inside the reactor for the total volume was calculated to be 0.8% H₂O.



Figure 8. Bubbler used to introduce humidity to CO₂ gas line. (photo by Daniel Piatek)

The voltage to the reactor was supplied by the Amazing1 PVM500 which is shown in Figure 9. The voltage applied ranged from 4kV to 7.5kV with a frequency of 25 kHz to 30 kHz. The voltage was monitored using a Tektronix P6015A high voltage probe. The voltage profile is shown below in Figure 7 as well.

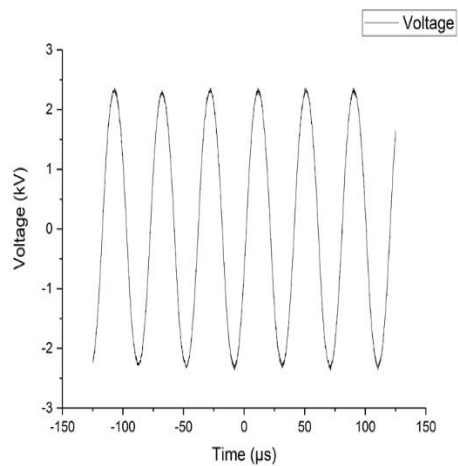


Figure 9. Power supply and voltage signal. (photo by Daniel Piatek)

Optical Emission Spectroscopy (OES) Setup:

OES was carried out using the Horiba iHR550 imaging spectrometer paired with the Princeton Instruments PI-Max 3 CCD camera. The 150 groove grating installed inside the spectrometer was used as the dispersive element to attain spectra. The slit of the spectrometer was kept at 0.05 mm. A 35 mm focal length focusing lens was setup between the spectrometer and reactor to concentrate the light onto the slit opening. This lens setup can be seen in Figure 5. This setup allowed for a resolution of 1.45Å/pix on the CCD camera.

Gas Mixtures and Experiments:

Table 1 shows the experiments that were carried out under various voltage and frequency settings along with a few different gas mixtures and flow rates. Tests 1 to 5 were carried out with an H₂/N₂ mixture of 25% and 75% respectively. The tests with CO₂ that was bubbled through an H₂O column were all at 0.8% water vapor for the reactor volume. Tests 11 and 12 were carried out using an Ar/CO₂ mixture of 87.5% and 12.50% respectively. Test 13 was performed using an H₂/He of 5% and 95% respectively.

Table 1. Experiments performed with various gasses and voltage settings.

Test #	Applied Voltage (kV)	Frequency (kHz)	Gas 1 (sccm)	Gas 2 (sccm)
1	5	24	H2/N2: 12.3	CO2: 10
2	4.75	25	H2/N2: 12.3	CO2: 10
3	5	30	H2/N2:25.6	CO2: 10
4	5	30	H2/N2: 49.3	CO2: 10
5	7.5	25	H2/N2: 12.3	CO2: 10
6	5.5	30	CO2/H2O: 3.2	N/A
7	5	25	CO2/H2O: 3.2	N/A
8	5	30	CO2/H2O: 3.2	N/A
9	7.5	25	CO2/H2O: 3.2	N/A
10	7.5	25	CO2: 3.2	N/A
11	5	25	Ar/CO2: 3.4	CO2/H2O: 3.2
12	4	25	Ar/CO2: 3.4	CO2/H2O: 3.2
13	5	25	H2/He: 7.3	CO2: 9.5

Results and Discussion

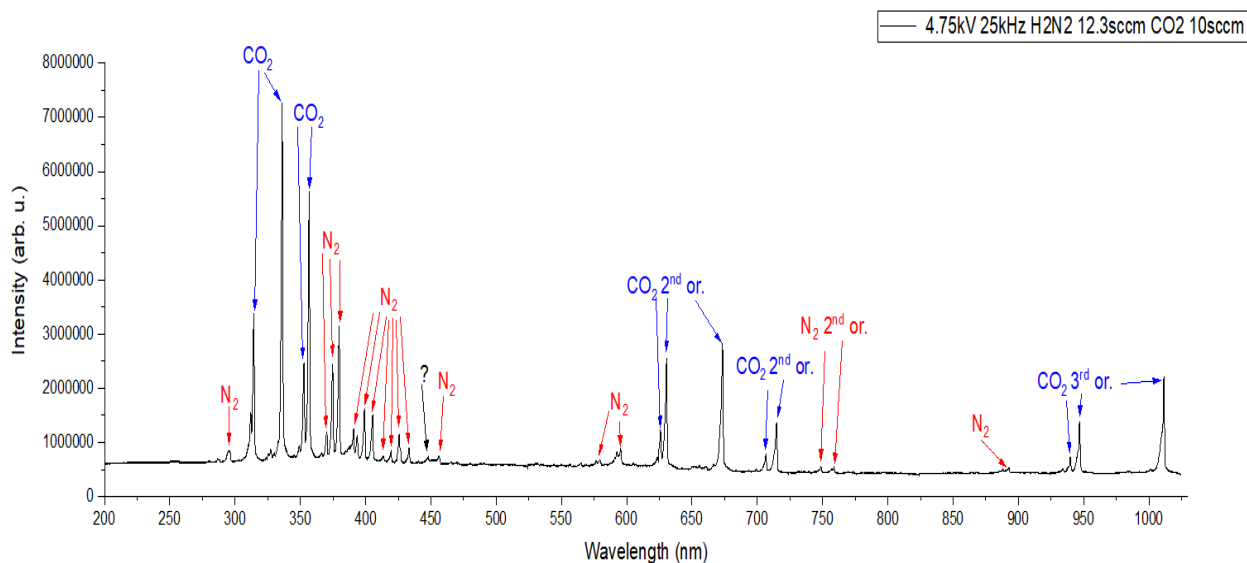


Figure 10. Typical optical emission spectrum

An example of an optical emission spectrum is shown above with labels for the different species generated. For any reader who wishes to get a clearer view of the full broadband spectra's from this work, Appendix 1 contains larger versions of the spectra's. The raw data is obtained from Matlab as individual scans which is then exported and stitched together in Origin to form a full broadband spectrum. The broadband spectrums were obtained using a 150 grooves/mm grating which allowed for a window of 148nm for each individual scan. This is coupled with an ICCD gate width of 100ms to avoid saturation of the ICCD itself and the accumulations would be varied by each scan to achieve the highest signal peak to noise ratio. The peaks that have been identified

and labeled agree well with what is found in the literature [1]. The following sections are grouped by gas composition for each experiment according to the table below.

Test #	Applied Voltage (kV)	Frequency (kHz)	Gas 1 (sccm)	Gas 2 (sccm)
1	5	24	H2/N2: 12.3	CO2: 10
2	4.75	25	H2/N2: 12.3	CO2: 10
3	5	30	H2/N2:25.6	CO2: 10
4	5	30	H2/N2: 49.3	CO2: 10
5	7.5	25	H2/N2: 12.3	CO2: 10
6	5.5	30	CO2/H2O: 3.2	N/A
7	5	25	CO2/H2O: 3.2	N/A
8	5	30	CO2/H2O: 3.2	N/A
9	7.5	25	CO2/H2O: 3.2	N/A
10	7.5	25	CO2: 3.2	N/A
11	5	25	Ar/CO2: 3.4	CO2/H2O: 3.2
12	4	25	Ar/CO2: 3.4	CO2/H2O: 3.2
13	5	25	H2/He: 7.3	CO2: 9.5

Table 1. Table of experiments

In order for methanol formation to occur, certain precursors must be present. The precursors and formation pathways for methanol from CO₂ are presented in figure 11 below. The two precursors that were looked for in this project are CH and OH which must be present in order for the formation of methanol to occur.

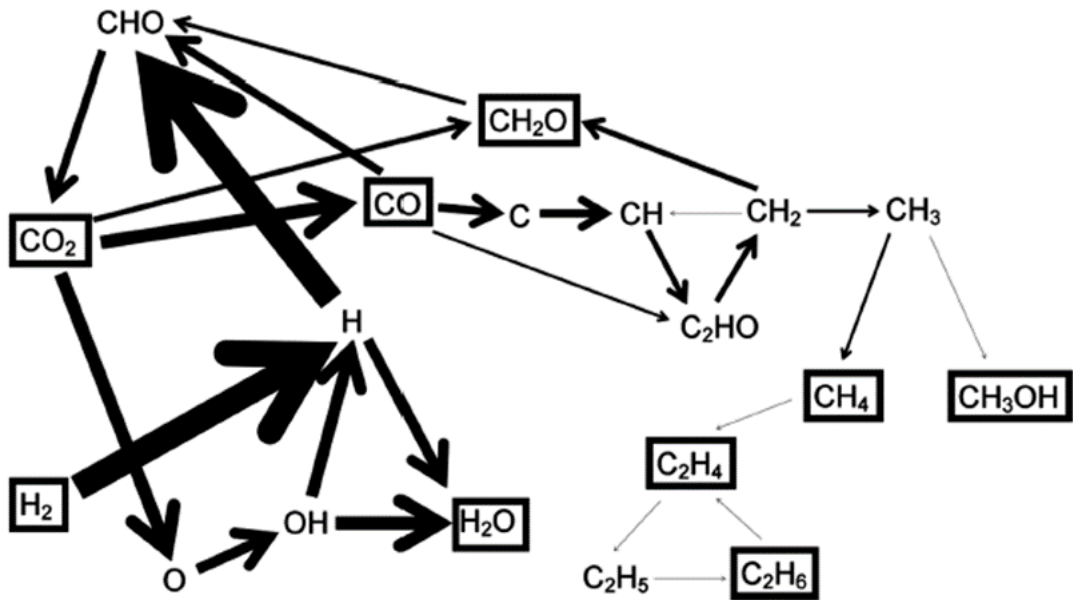


Figure 11. Reaction pathways for the conversion of CO₂ and H₂ to methanol and other products. [2]

Section 4.1: H₂/N₂ and CO₂

Below are the broadband spectrums for all of the H₂/N₂ (25%/75%) with CO₂ experiments conducted. Multiple runs were done with this gas composition to study the effect of flow rate, voltage applied, and frequency on the species generated within the plasma. N₂ was chosen in these experiments as it was shown by Wang *et al.* [3] that the presence of N₂ in a CO₂ plasma increases the overall conversion rate. This is attributed to the N₂ metastable states which help with dissociation of the CO₂ molecule.

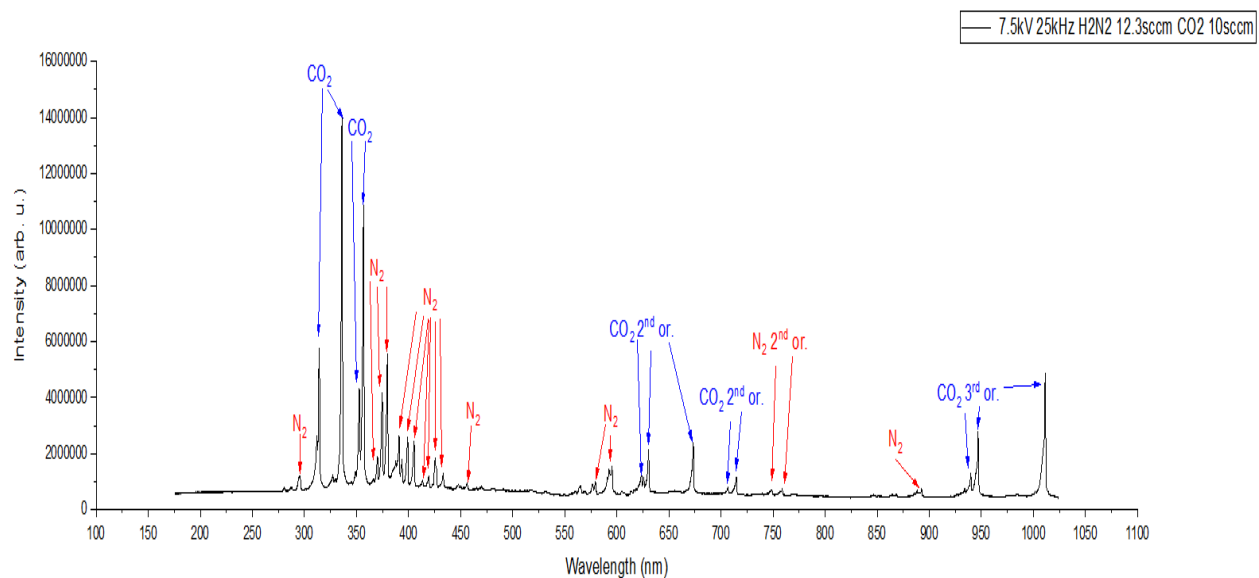
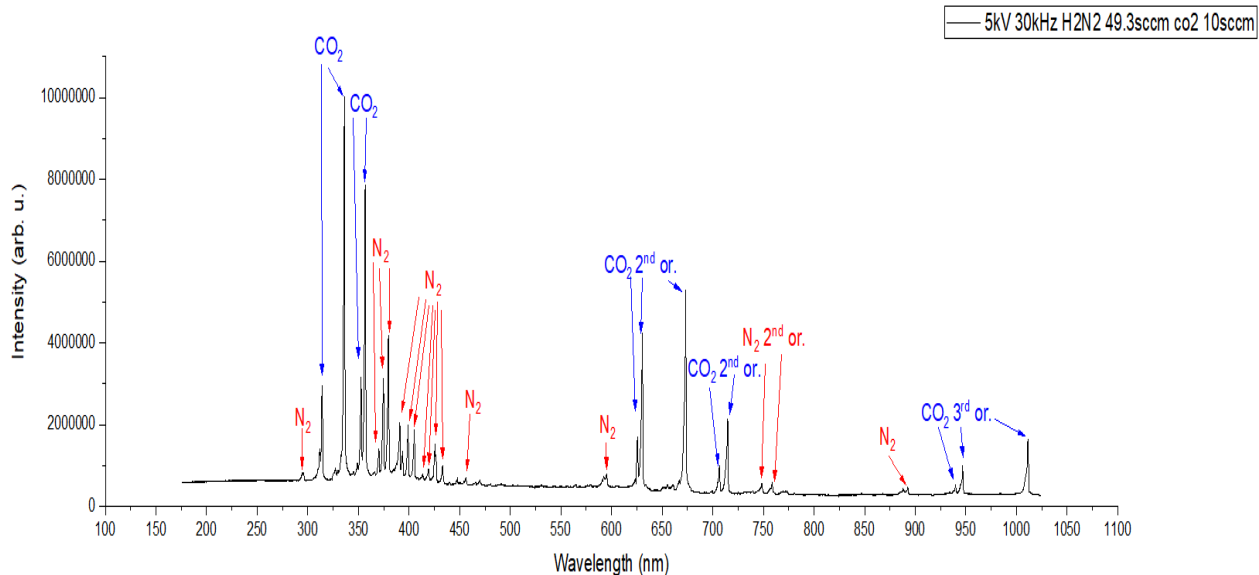


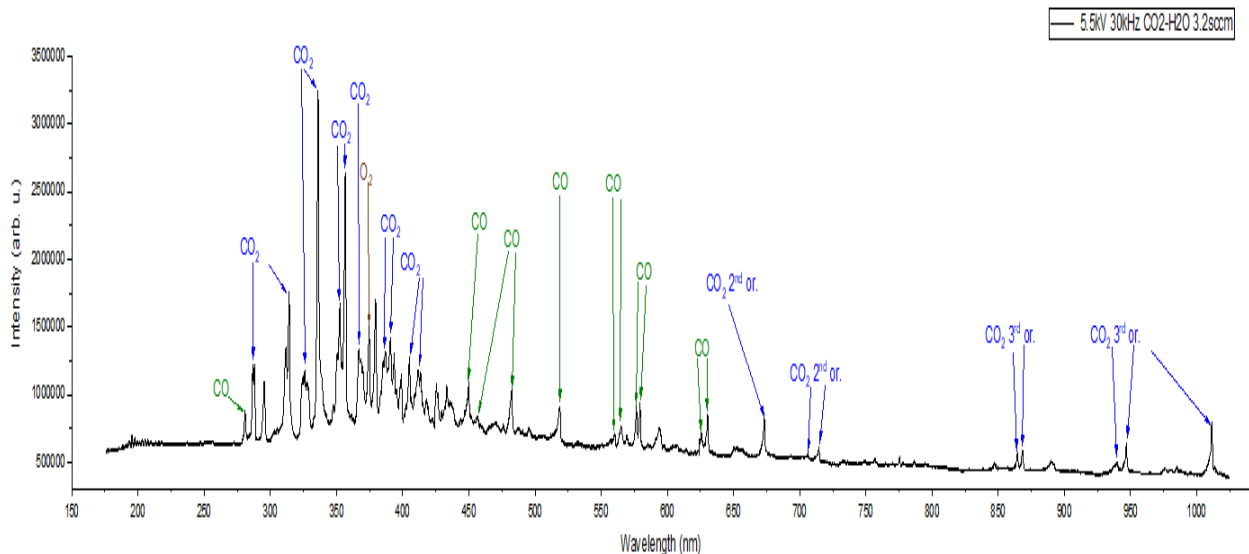
Figure 12. Spectra from the H₂/N₂ with CO₂ experiments conducted using different applied voltage, frequency, and flow rate. (CO₂=blue, N₂=red)

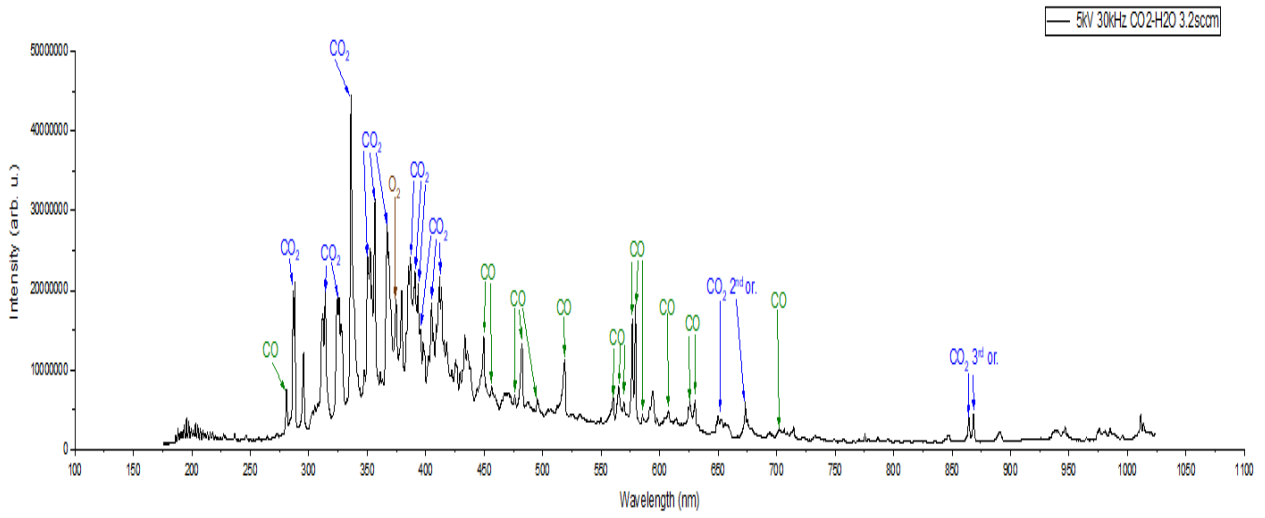
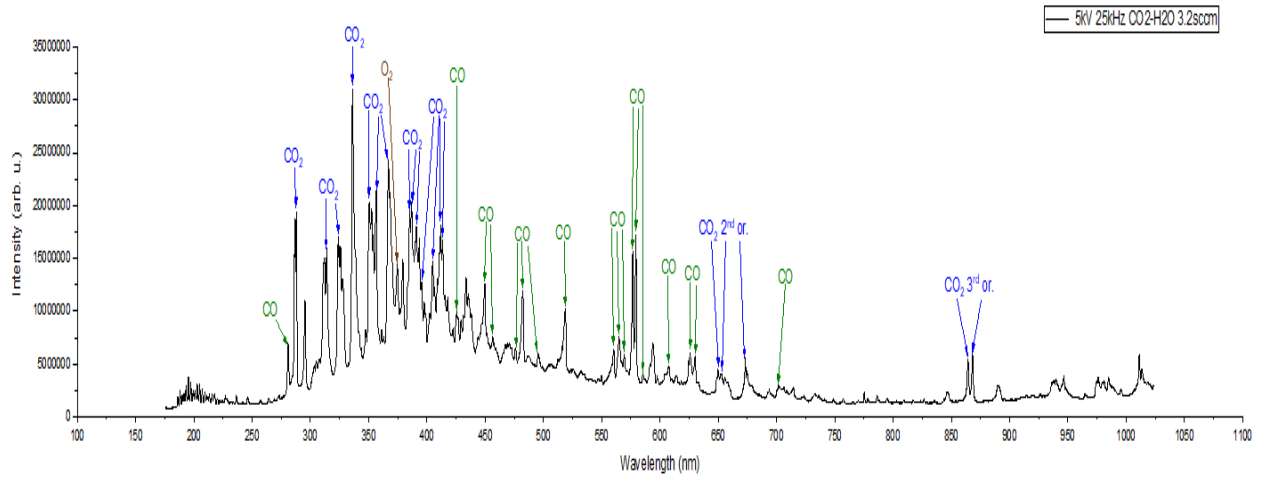
As can be seen from the different spectra's shown above, CO₂ and N₂ excitation was observed. The largest peak seen in these spectra is attributed to CO₂ at 336nm. Other major lines of CO₂ from the spectra were at 314nm, 350nm, and 356nm. N₂ lines were also present in these

spectra at 371nm, 375nm, 380nm, 389nm, 399nm, 405nm, 426nm, and 595nm which is expected. No lines corresponding to CH or OH formation were observed in the spectra's. Also, no emission lines of H₂ were observed in these experiments.

Section 4.2: CO₂ and H₂O

Next, the spectra for the CO₂ and H₂O experiments are shown below. H₂O vapor was introduced to the reactor by bubbling CO₂ through a water column at a constant flow rate. The water vapor content in the reactor was calculated to be 0.8% H₂O for the total volume of the reactor using the Antoine equation. The H₂O vapor content was kept constant for all the experiments conducted using water vapor. Applied voltage and frequency were varied throughout these experiments to understand their impact on species generation within the plasma discharge.





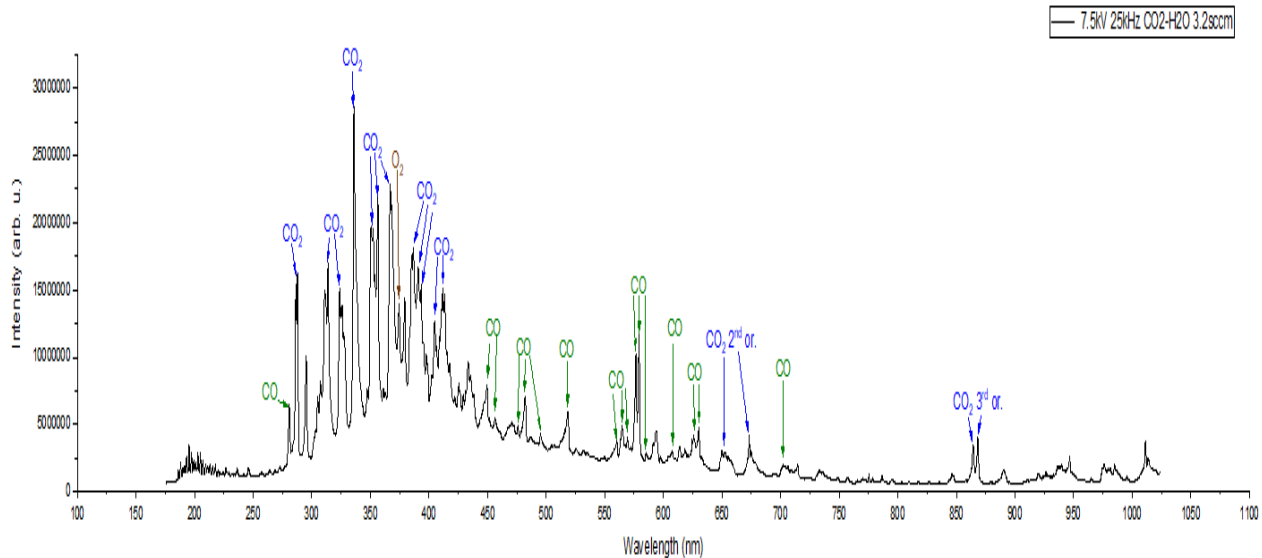


Figure 13. Spectra from the CO₂ with H₂O vapor experiments conducted using different applied voltage and frequency. (CO₂=blue, CO=green, O₂=brown).

The spectra from these experiments show that CO₂ dissociation was achieved. This is evidenced by the appearance of CO emission lines at 451nm, 483nm, 519nm, 575nm, 578nm, and 631nm. Additionally, an O₂ emission line was observed at 374nm which could only form due to CO₂ dissociating into CO and O. Unfortunately, no CH or OH lines were found in these spectra as well. Varying the applied voltage and frequency did not result in any new emission lines being generated.

Section 4.3: Pure CO₂

A pure CO₂ test was conducted to understand the species generated. It also allowed a direct comparison to be done between pure CO₂ and other gas mixtures in the reactor. This test was conducted with an applied voltage of 7.5kV and a frequency of 25kHz while flowing the CO₂ at 3.2sccm. Below is the full spectrum for the pure CO₂ experiment.

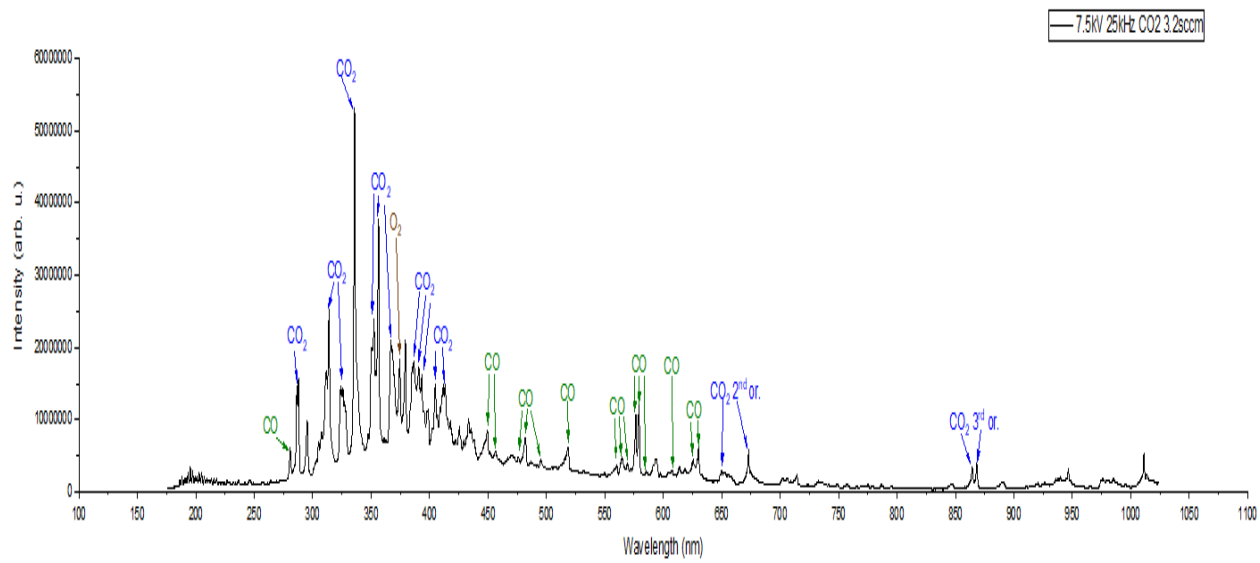


Figure 14. Spectrum of the pure CO₂ experiment. (blue=CO₂, green=CO, brown=O₂)

Emission lines of CO₂ were present at 287nm, 314nm, 324nm, 337nm, 356nm, 366nm, 377nm, and 405nm. Pure CO₂ resulted in CO₂ dissociation. This is shown by the emission lines of CO at 280nm, 451nm, 483nm, 519nm, 581nm, and 630nm. This also resulted in the formation of O₂ which produced an emission line at 374nm.

Section 4.4: Argon and CO₂ with H₂O

A mixture of Ar/CO₂(87.5%/12.5%) was introduced to the reactor because of previous work conducted by Ramakers *et al.*[4] that showed improvement in CO₂ conversion with the addition of argon to a CO₂ plasma discharge. The applied voltage was varied to study its effect on the species generated. The amount of water vapor in the line was kept constant as with previous experiments at 0.8% the total volume of the reactor. Flow rates and applied frequencies were kept constant. The resulting spectra's are presented below in figure 6.

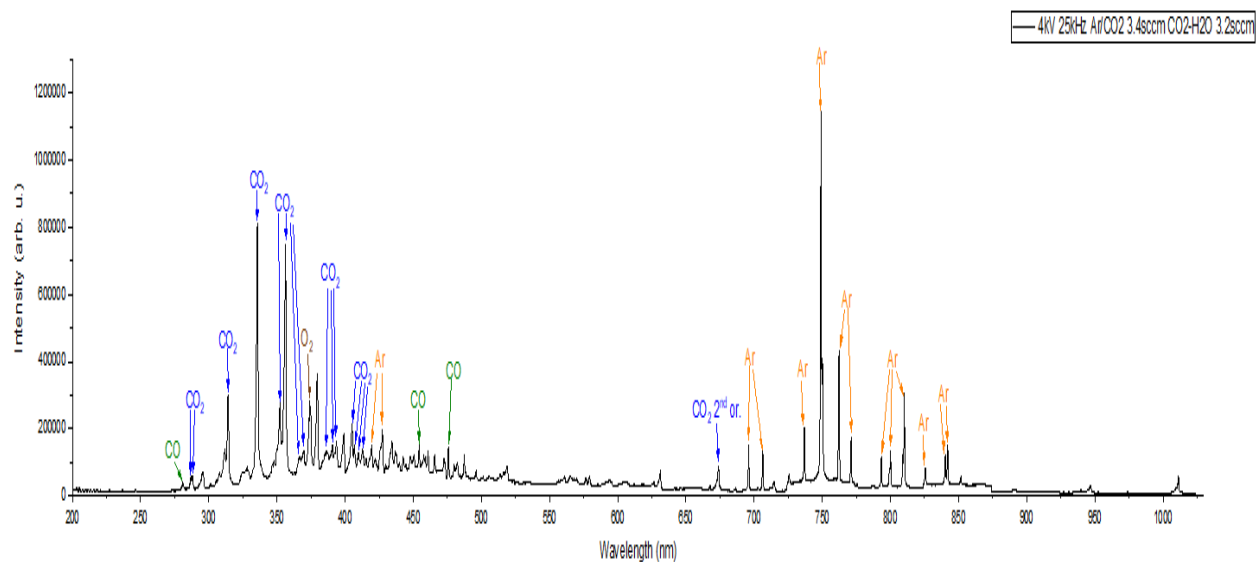
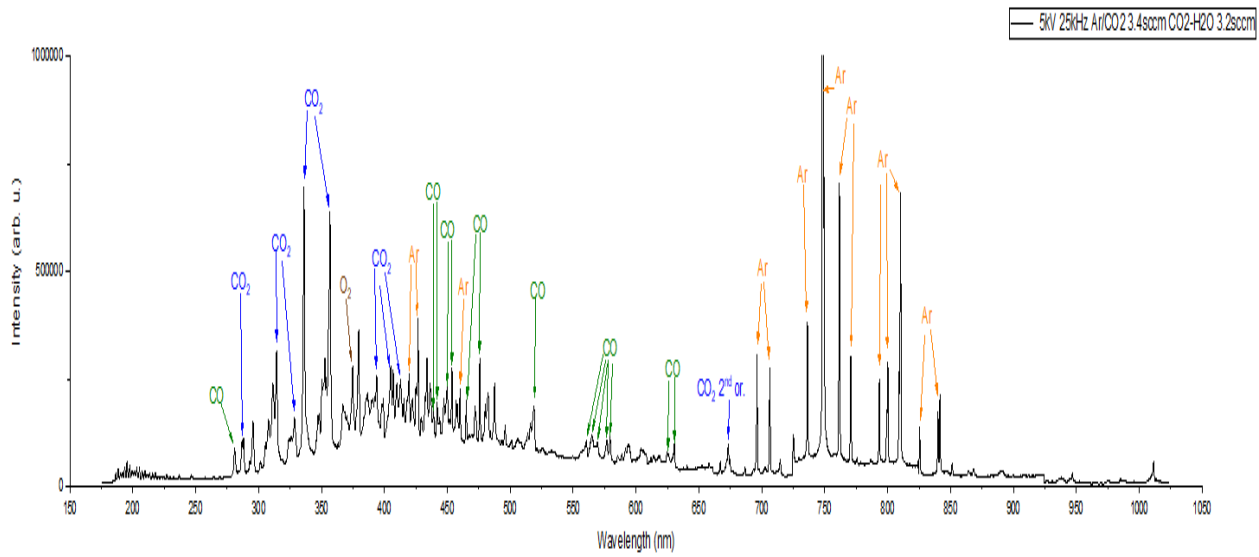


Figure 15. Emission spectra of the Ar/CO₂/H₂O experiments. (blue=CO₂, green=CO, orange=Ar, brown=O₂)

As seen previously, CO₂ emission lines are visible at 287nm, 314nm, 324nm, 337nm, 356nm, and 405nm. CO₂ dissociation was achieved as evidenced by the emission lines of CO being

present as well as the emission line of O₂. Additionally, argon emission lines were present at 419nm, 426nm, 696nm, 750nm, 763nm, 772nm, 794nm, 800nm, 810nm, and 826nm.

Section 4.5: Helium/Hydrogen with CO₂

It was reported by Ramakers *et al.*[4] that the addition of helium into a CO₂ plasma increases the conversion rate due to a lower breakdown voltage which allows for a larger fraction of the applied power to convert CO₂. An experiment using a He/H₂(95%/5%) gas mixture along with CO₂ was conducted in order to observe the influence helium has on the species generated within the plasma discharge. Applied voltage was kept at 5kV with a frequency of 25kHz. The He/H₂ gas was fed into the reactor at 7.3sccm while the CO₂ gas was flowing at 9.5sccm. The resulting emission spectrum is shown below.

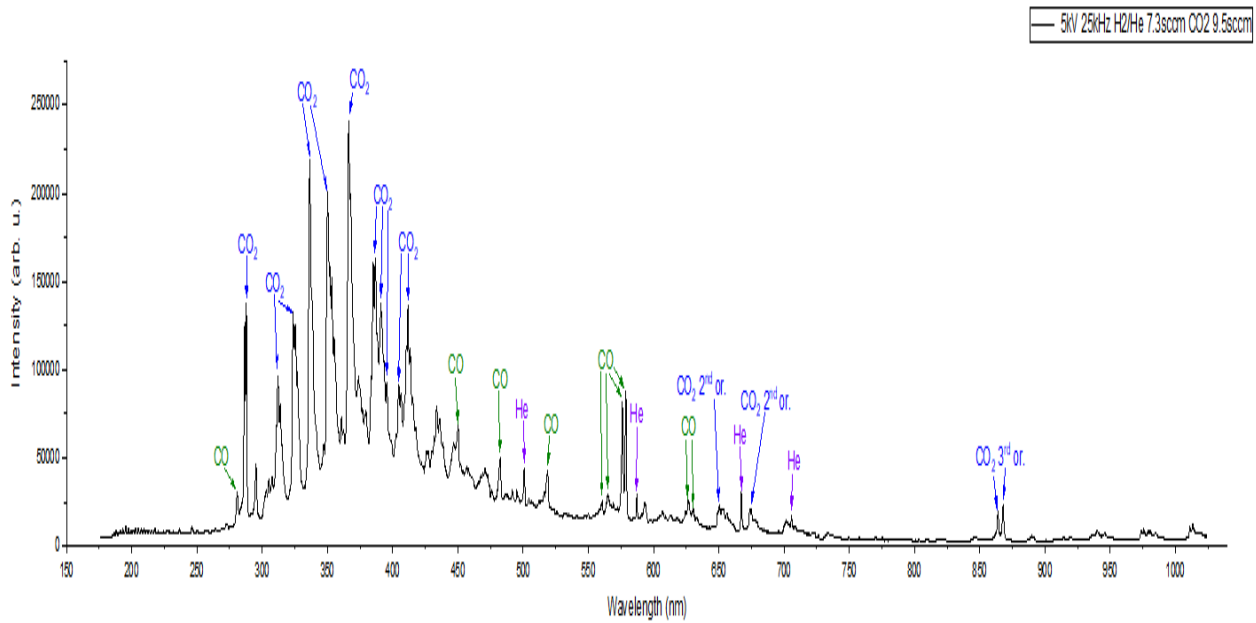


Figure 16. Emission spectrum of H₂/He with CO₂. (blue=CO₂, green=CO, purple=Helium)

As can be seen from the emission spectrum above, CO₂ emission lines were present at 287nm, 313nm, 324nm, 337nm, 350nm, 366nm, 387nm, and 412nm as would be expected. Additionally, CO₂ dissociation was achieved as evidenced by the presence of the CO lines at 280nm, 451nm, 483nm, 519nm, and 578nm. Furthermore, helium lines were present at 501nm, 587nm, 667nm, and 706nm. As with previous experiments, there were no emission lines indicating either CH or OH formation. There was also a lack of any hydrogen lines.

Section 4.6: Comparison and Discussion

A comparison in the emission spectrums between experiments 7 and 11, from the table above, shows the appearance of a new emission line at 476nm with using argon in the reactor. This emission line corresponds to a CO emission line. The appearance of this emission line may point to an increase in CO₂ dissociation. While CO₂ dissociation is a good step towards the end goal of this research, the lack of OH and CH emission lines in any of the emission spectrum is still an issue. The lack of OH and CH lines may be explained by a competing back reaction of the CO molecules back into CO₂ as this is more thermodynamically favorable. Additionally, the energy required for CO₂ dissociation into CO is in the area of $\approx 5.5\text{eV}$ while the energy required for the dissociation of CO into oxygen and carbon requires $\approx 11.1\text{eV}$. The energy required for CO dissociation to occur and CH or OH formation to occur may not be present in this type of cold plasma. This issue could be tackled with the use of a catalyst to lower the energy required for these reactions to occur as all these experiments were done in a regular DBD setup and did not include a catalytic material. The absence of any strong hydrogen lines is also troublesome, in the experiments that utilized water vapor, as this points to a lack of dissociation of water vapor thus

also preventing the formation of any CH or OH species. Also, a higher resolution emission spectrum may need to be performed to look in the 300nm to 400nm region as the OH emission lines may have been blended in with the CO₂ emission lines and thus making them difficult to distinguish on these broadband spectra.

Conclusion

The hydrogenation of carbon dioxide (CO_2) into methanol (CH_3OH) is a promising route for utilizing excess CO_2 to create a useful product. Additionally, using water vapor instead of pure H_2 gas and being able to utilize this process at atmospheric pressure would make this process much more cost efficient for real world implementation. In this project, the dissociation of CO_2 was achieved into carbon monoxide (CO). However, further conversion of CO into CH was not successful. This is probably due to CO converting back into CO_2 . Experiments utilizing argon did show some improvement in CO_2 to CO conversion. Also, further investigation of this system with higher resolution spectroscopy may yield more information on species generated within the plasma discharge as the 300 nm to 400 nm region is quite packed with emission lines from CO_2 and some lines may have been missed due to their lower intensity or blending with stronger lines in the same region. Coincidentally, this is also the region where OH would have had emission lines. Furthermore, coupling this system with a suitable catalyst to assist in the conversion of CO_2 may bring interesting results.

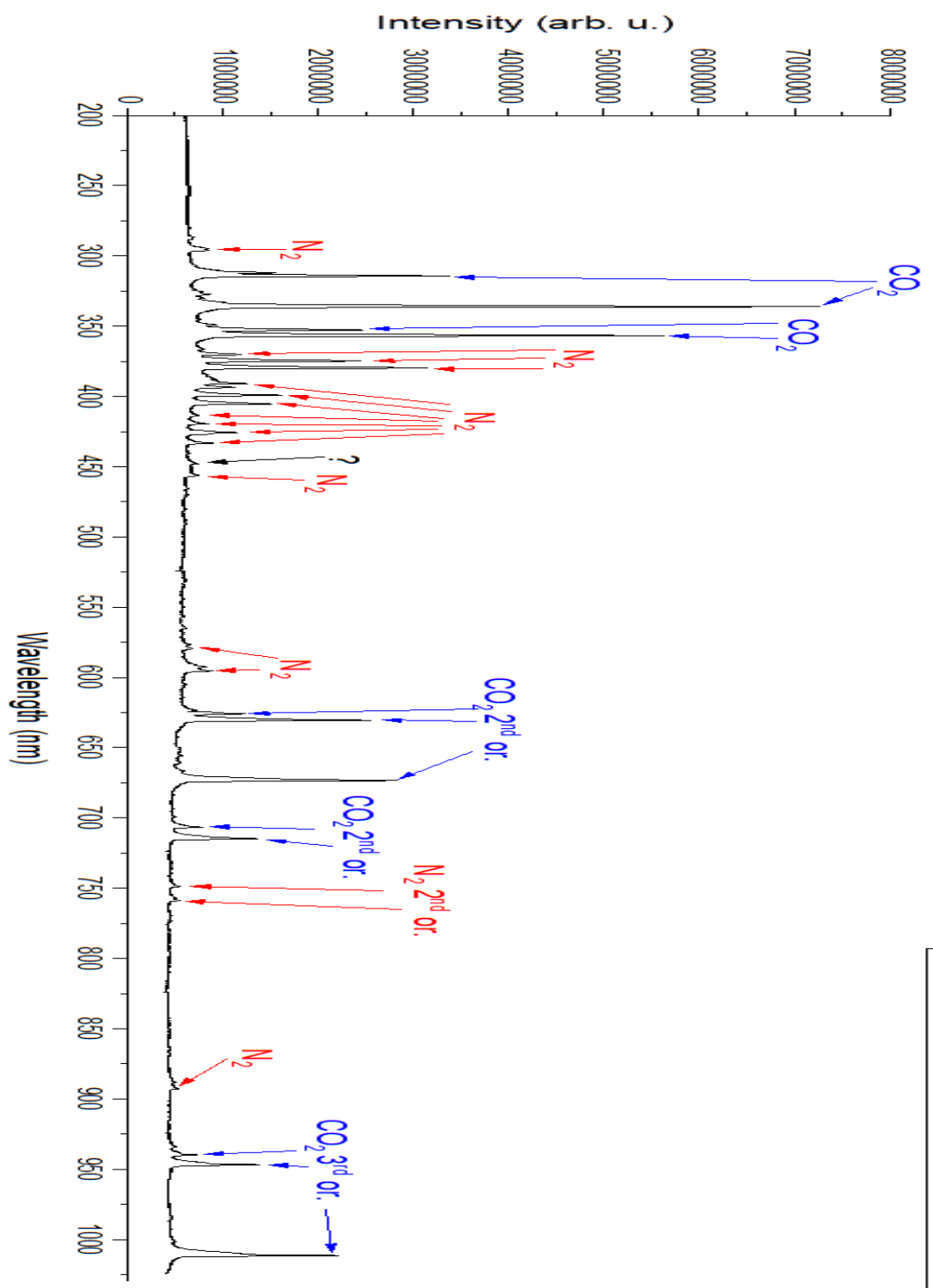
References

1. Kim, H., Teramoto, Y., Ogata, A., Takagi, H., & Nanba, T. (2015). Plasma Catalysis for Environmental Treatment and Energy Applications. *Plasma Chemistry and Plasma Processing*, 36(1), 45-72. doi:10.1007/s11090-015-9652-7
2. Nozaki, T., & Okazaki, K. (2013). Non-thermal plasma catalysis of methane: Principles, energy efficiency, and applications. *Catalysis Today*, 211, 29-38. doi:10.1016/j.cattod.2013.04.002
3. Tu, X., Whitehead, J. C., & Nozaki, T. (2019). *Plasma catalysis: Fundamentals and applications*. Cham: Springer.
4. Carreon, M. L. (2019). Plasma catalysis: A brief tutorial. *Plasma Research Express*, 1(4), 043001. doi:10.1088/2516-1067/ab5a30
5. Dielectric barrier discharge. (2020, July 23). Retrieved July 28, 2020, from https://en.wikipedia.org/wiki/Dielectric_barrier_discharge
6. How does a plasma TV work? (2020, February 26). Retrieved July 28, 2020, from <https://www.explainthatstuff.com/plasmatv.html>
7. Fridman, A. A., & Kennedy, L. A. (2020). *Plasma physics and engineering*. Boca Raton, FL: CRC Press.
8. Bogaerts, A., Bie, C. D., Snoeckx, R., & Kozák, T. (2016). Plasma based CO₂ and CH₄ conversion: A modeling perspective. *Plasma Processes and Polymers*, 14(6), 1600070. doi:10.1002/ppap.201600070
9. Ramakers, M., Michiels, I., Aerts, R., Meynen, V., & Bogaerts, A. (2015). Effect of Argon or Helium on the CO₂ Conversion in a Dielectric Barrier Discharge. *Plasma Processes and Polymers*, 12(8), 755-763. Doi:10.1002/ppap.201400213.

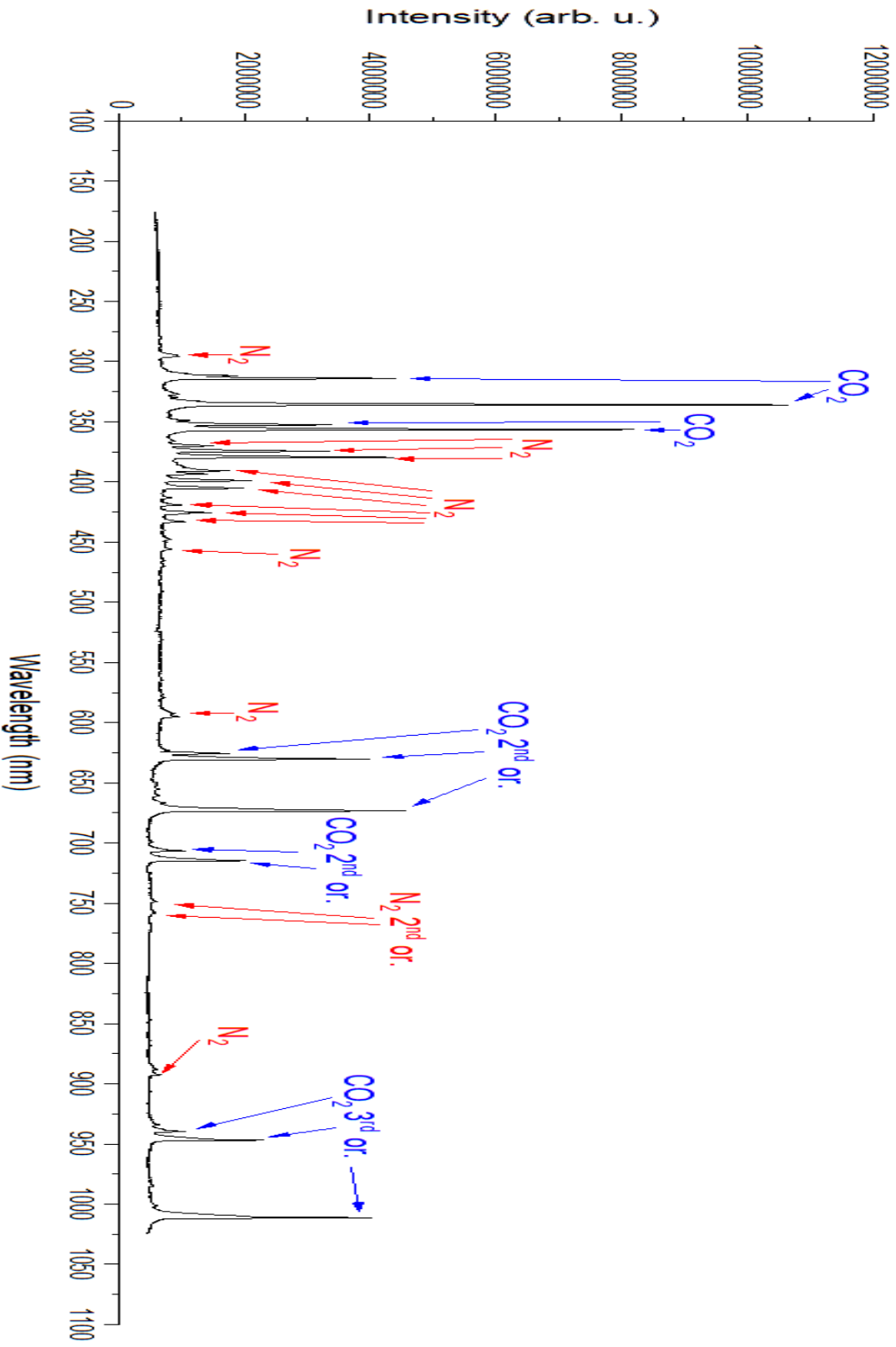
10. Tahir, M. (2016). Selective Photocatalytic Reduction of CO₂ by H₂O/H₂ to CH₄ and CH₃OH over Cu-Promoted In₂O₃/TiO₂ Nanocatalyst. Amsterdam, Netherlands: Applied Surface Science.

Appendix 1

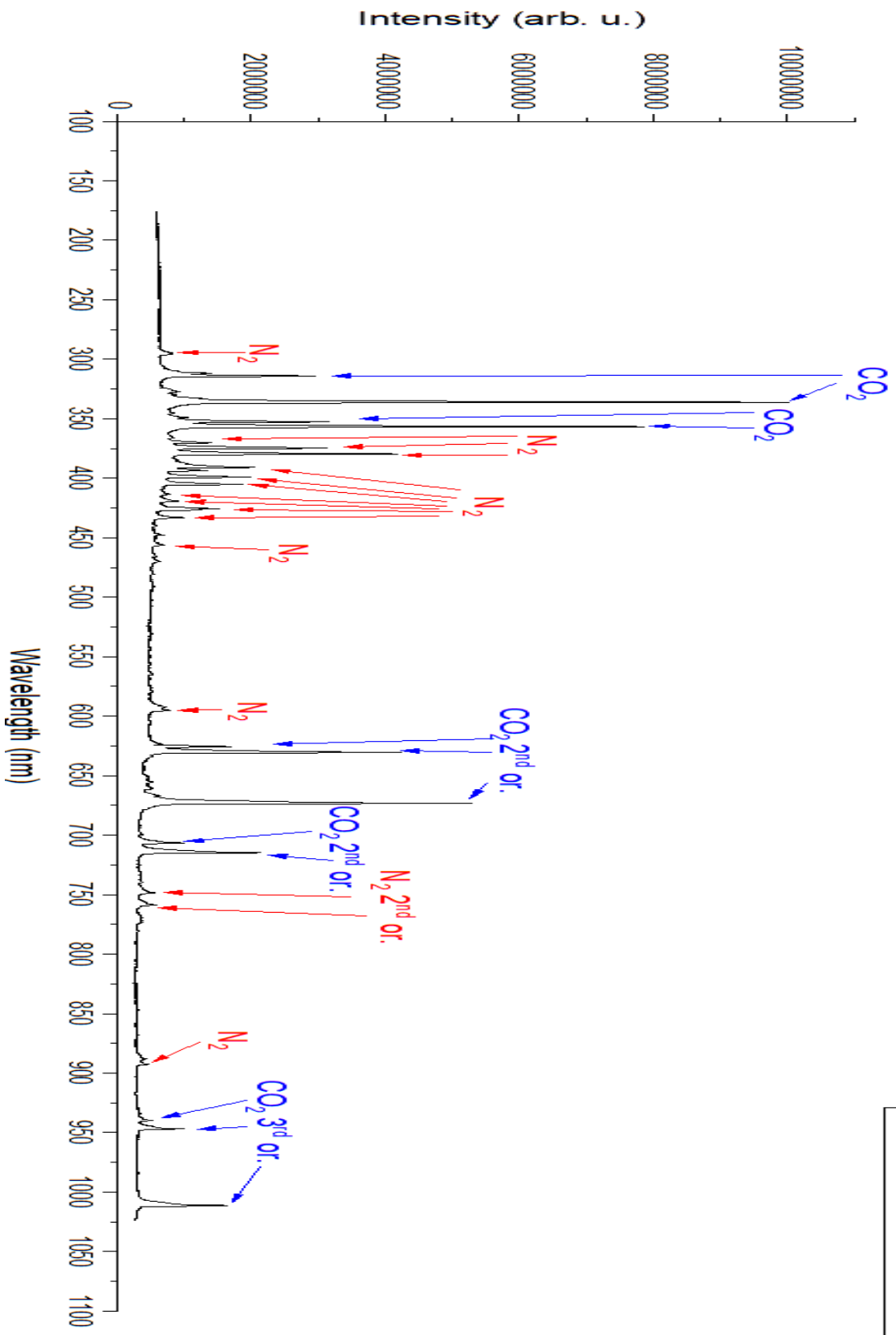
— 2 19 2020 4.75kV 25kHz H2N2 12.3sccm CO2 10sccm



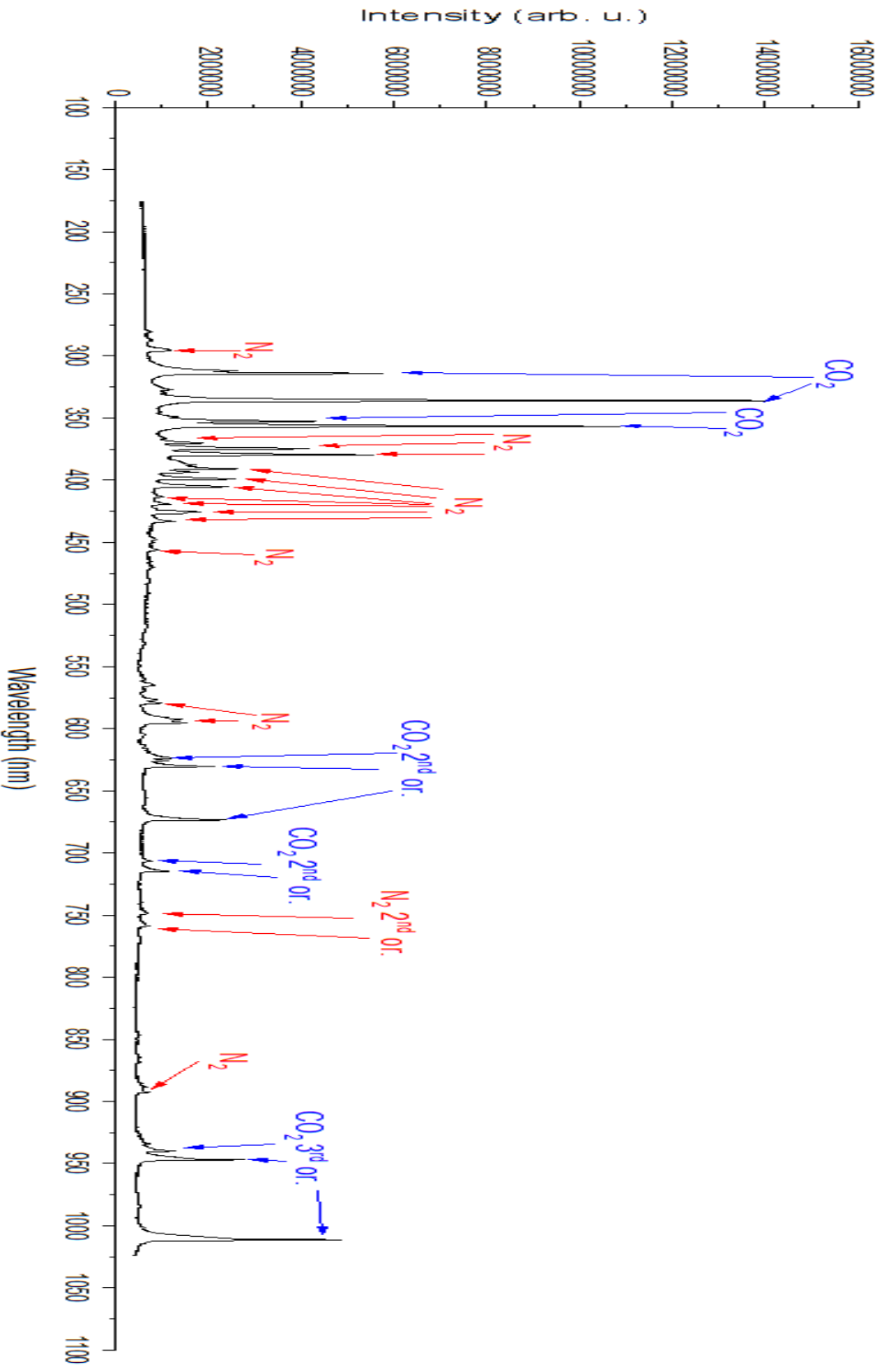
— 5kV 30kHz H2N2 25.6scm CO2 10scm

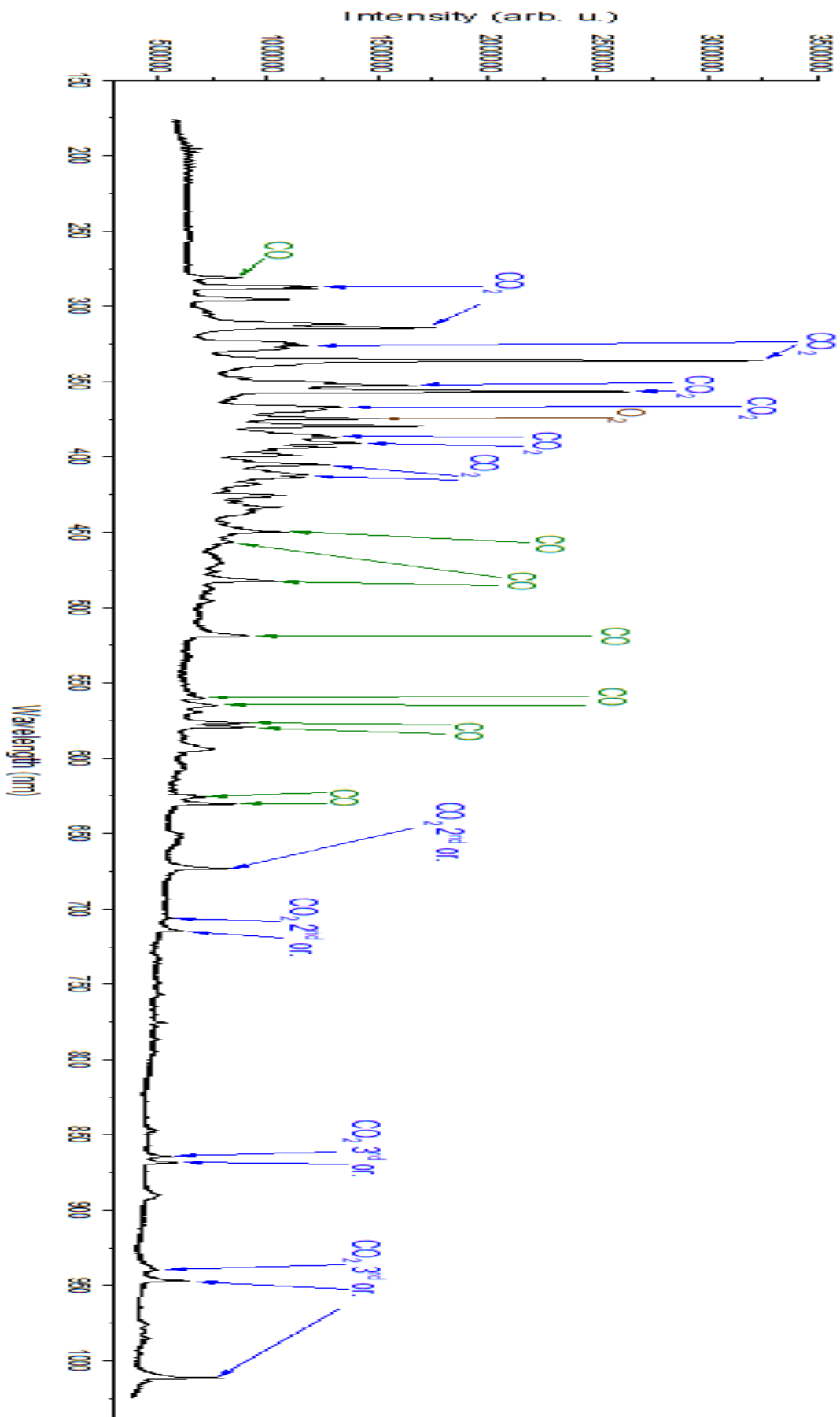


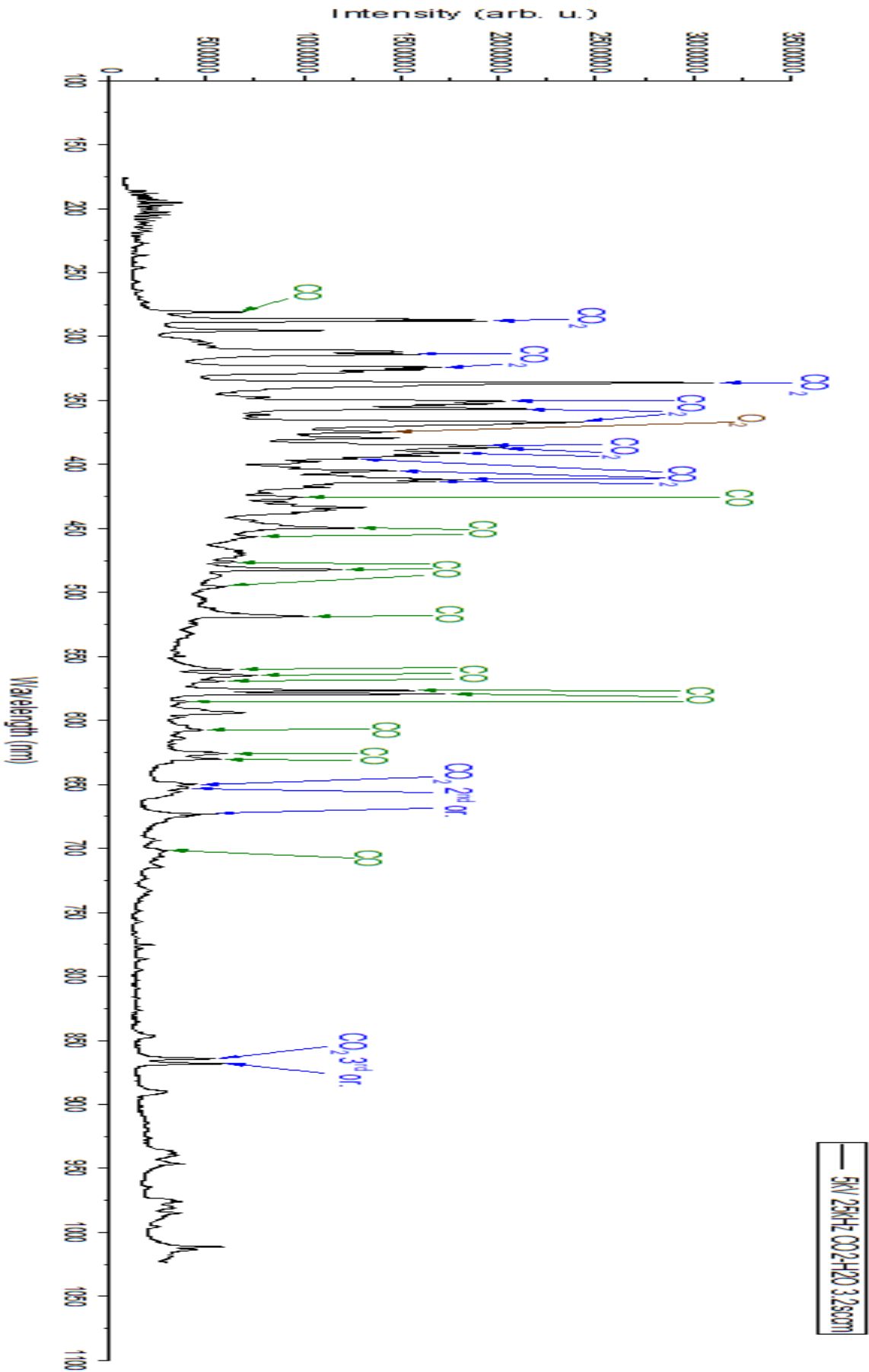
— 5kV 30KHz H2N2 49.3scm CO2 10scm



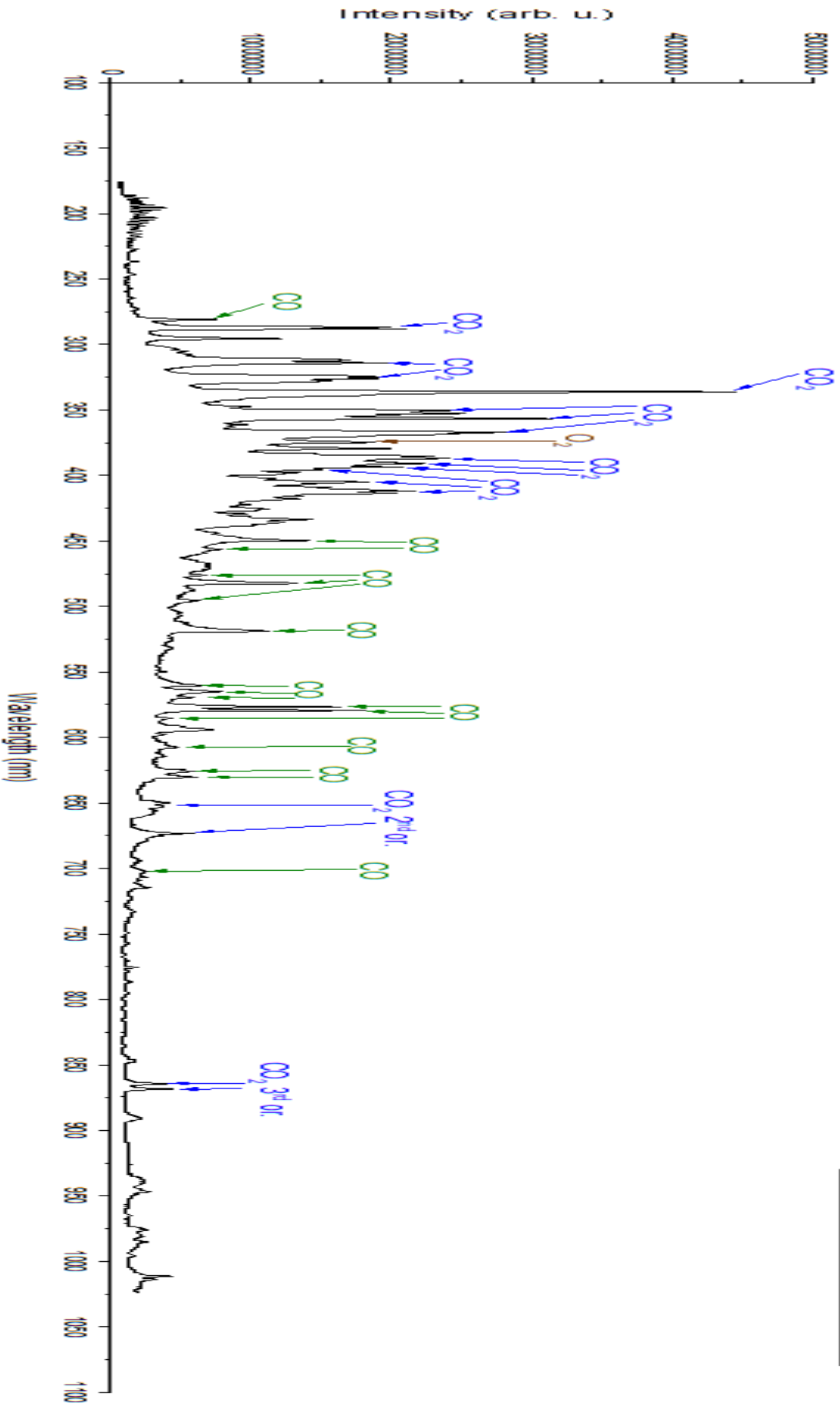
7.5kV 25kHz H2N2 12.3sccm CO2 10sccm

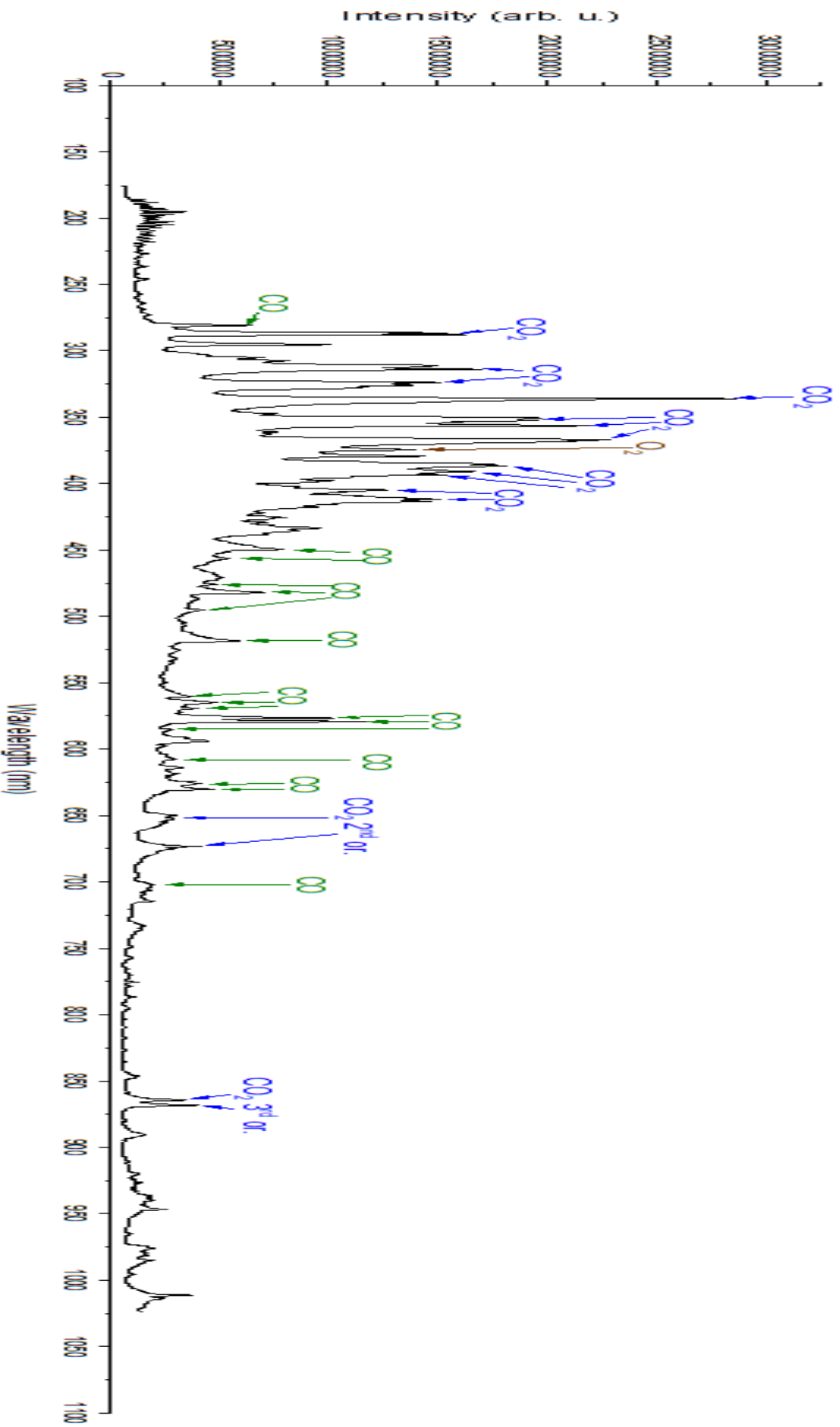


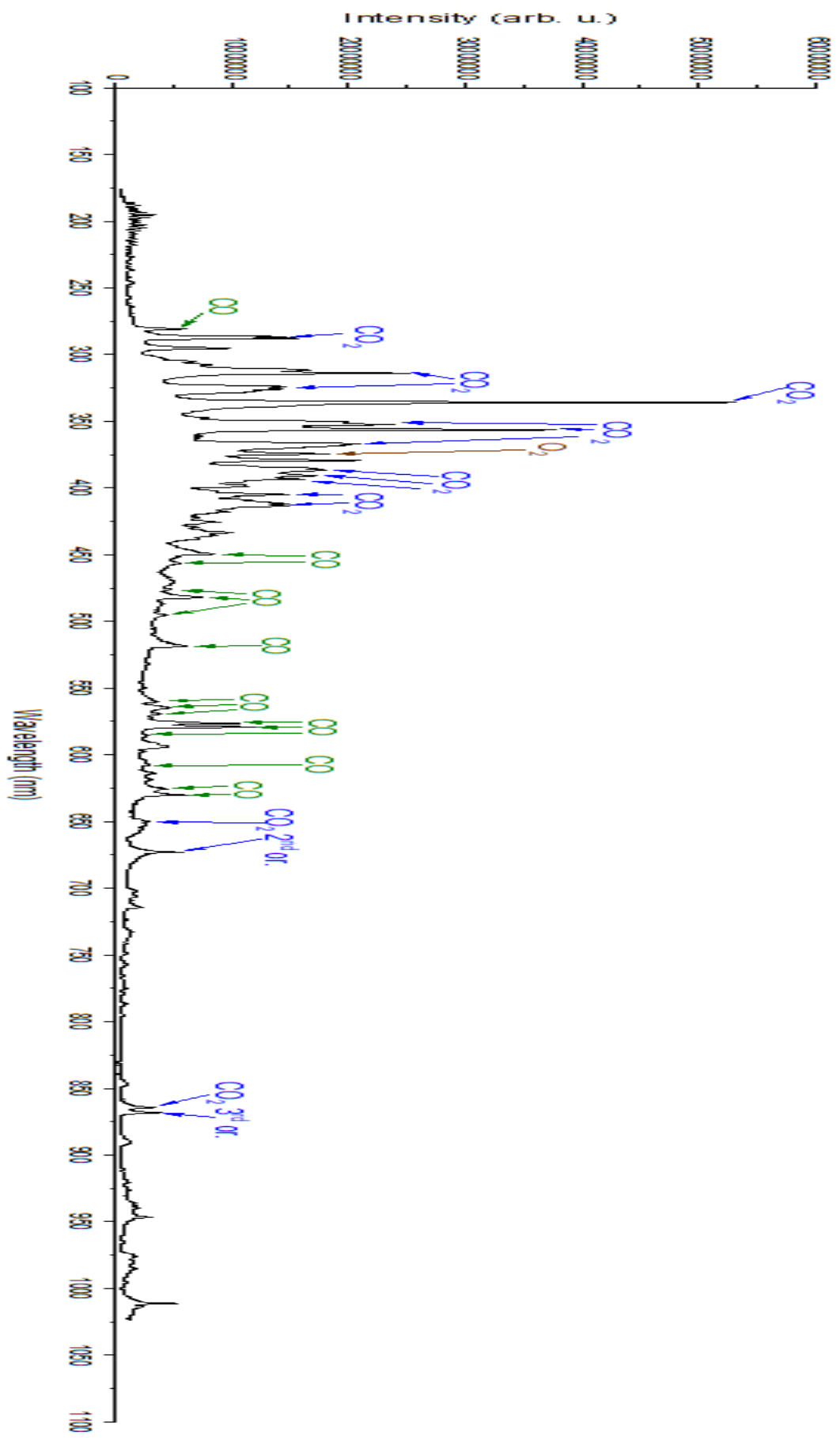




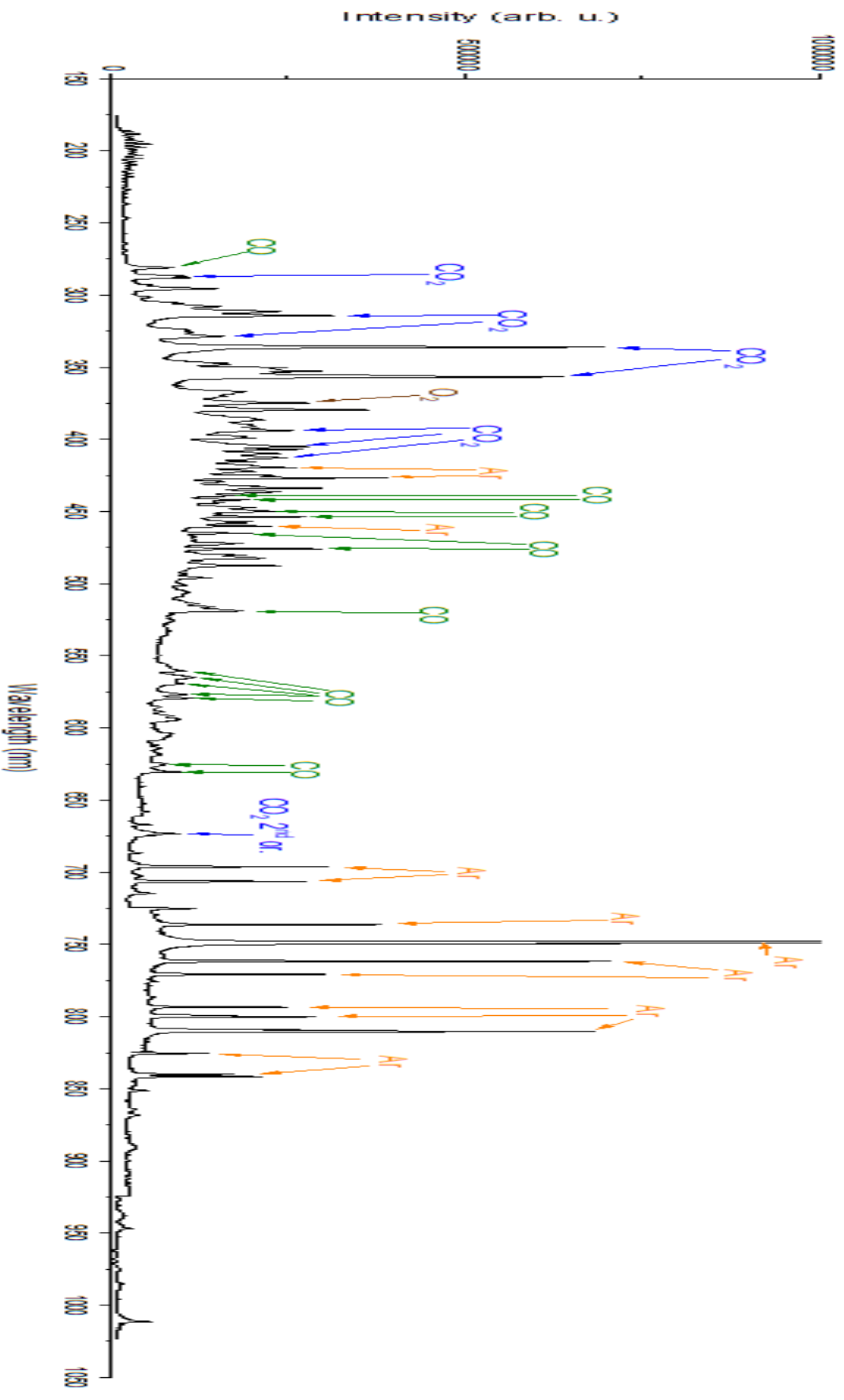
5W 30kHz CO2+H2O 3.250nm

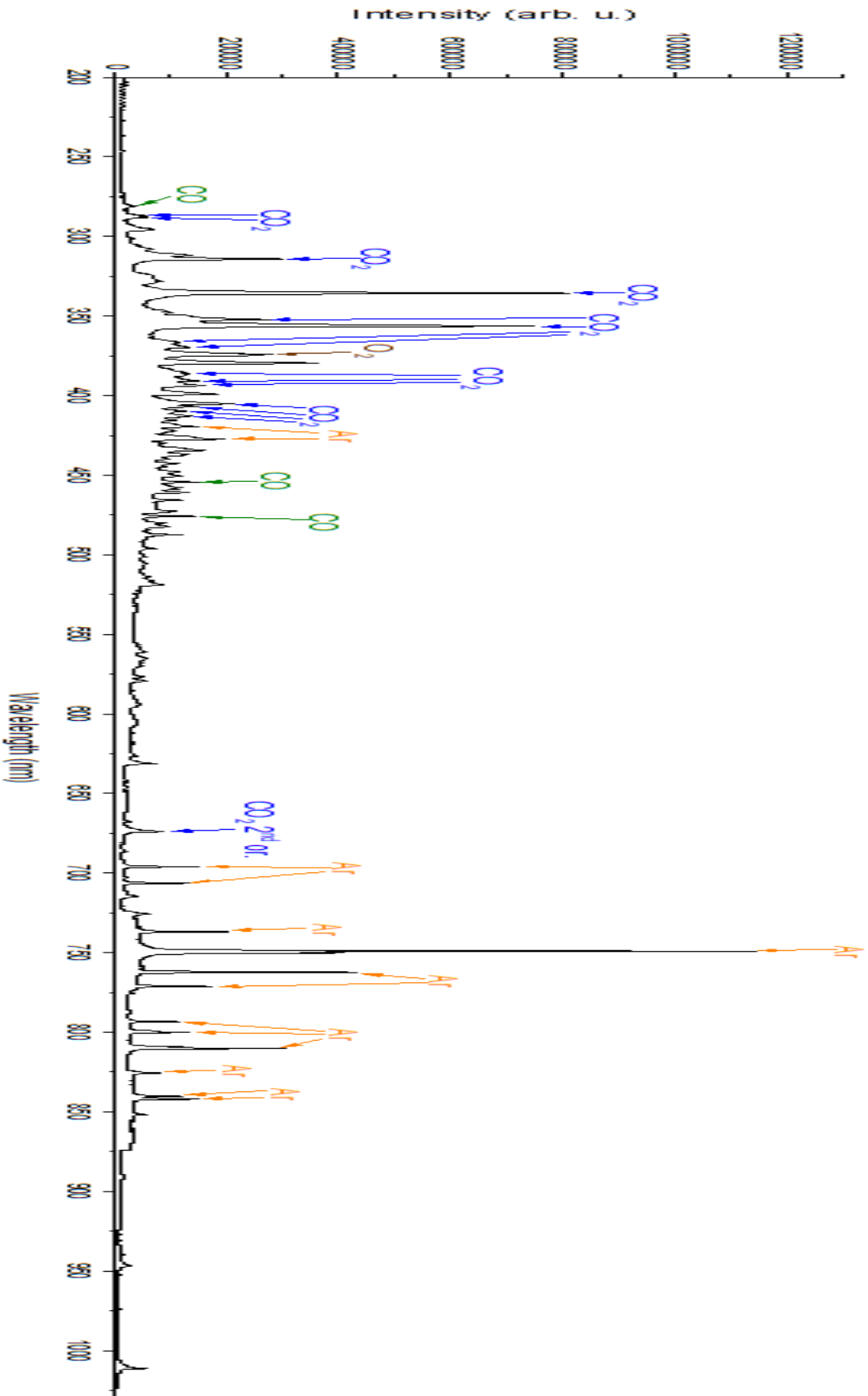




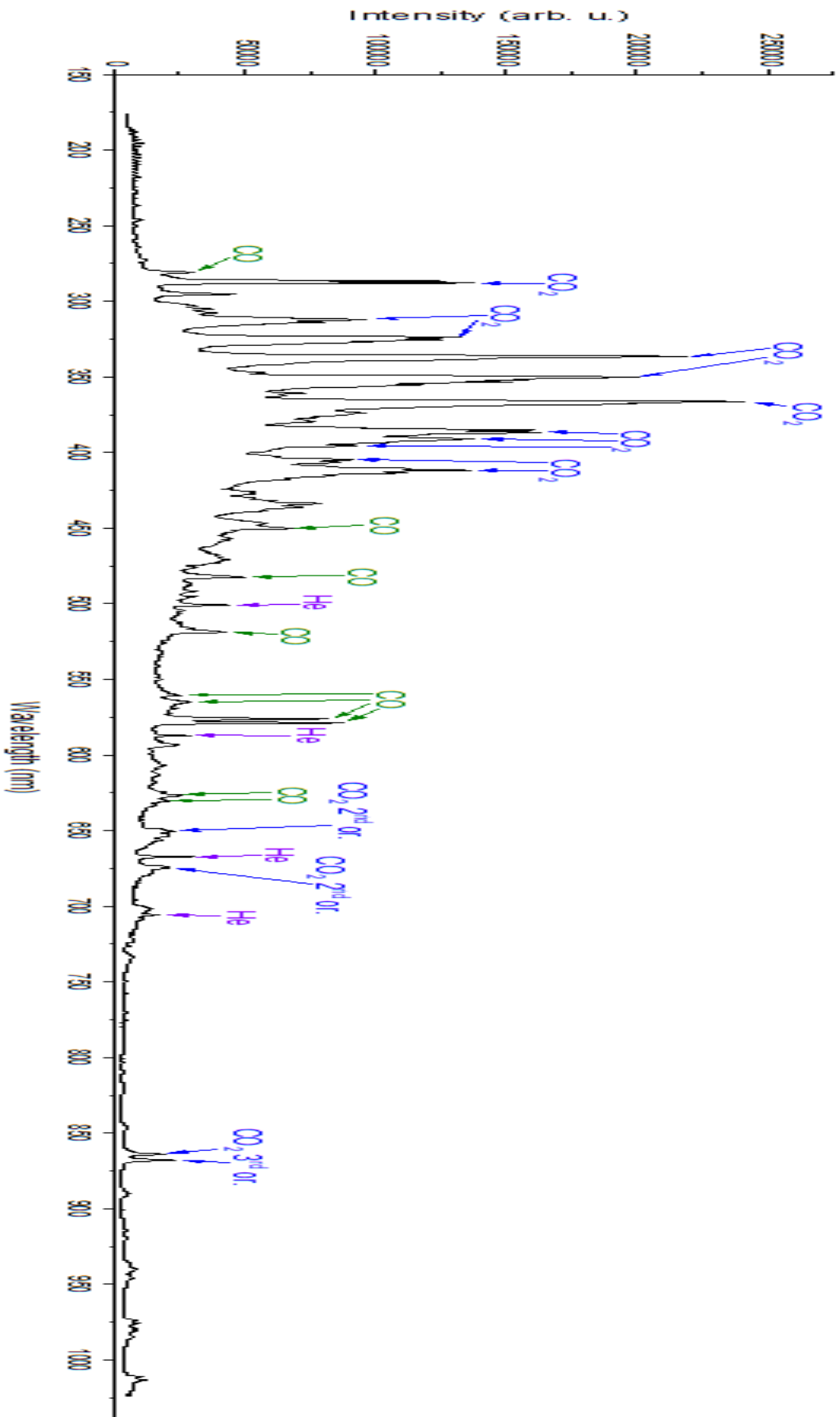


— 7.5W ZENITH CO2 3.280cm





4K1 251Hz ArCO2 3.450cm CO2H2O 3.250cm



5N/25NHe H2He 7.35cm CO2 9.55cm